ACS OMEGA

http://pubs.acs.org/journal/acsodf

Article

Small Peptides Targeting BACE-1, AChE, and A-β Reversing Scopolamine-Induced Memory Impairment: A Multitarget Approach against Alzheimer's Disease

Baljit Kaur, Rajbir Kaur, Vivesh, Sudesh Rani, Rajbir Bhatti, and Palwinder Singh*

Cite This: *ACS Omega* 2024, 9, 12896−12913

Read Online

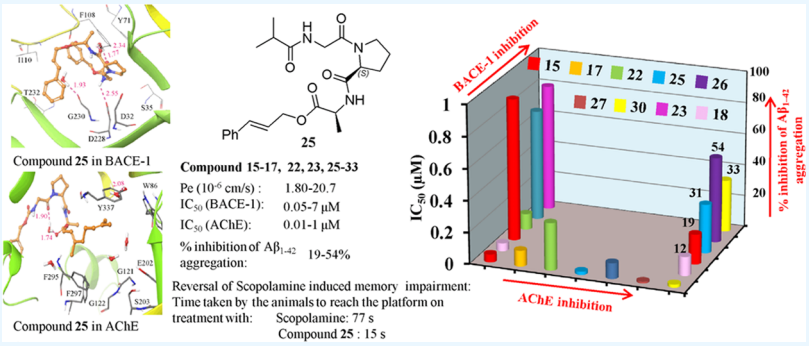

ABSTRACT: Based on the biochemical understanding of Alzheimer's disease, here, we report the design, synthesis, and biological screening of a series of compounds against this neuro-disorder. Adopting the multitarget approach, the catalytic processes of BACE-1 and AChE were targeted, and thereby, compounds **15**, **22**, **25**, **26**, **27**, and **30** were identified with IC_{50} in the submicromolar range against these two enzymes. Further, compounds **15** and **25** displayed more than 50% inhibition of β-amyloid aggregation. Implying their physiological use, the compounds exhibited appreciable biological membrane permeability as observed through the parallel artificial membrane permeability experiment. Supporting these results, treatment of the mice with the test compounds reversed their scopolamine-affected memory impairment, where the highest healing effect was seen in the case of compound **25**. Overall, the combination of molecular modeling and experimental studies provided highly effective molecules against Alzheimer's disease.

1. INTRODUCTION

Neuro-degenerative disorders including Parkinson's disease, Alzheimer's disease, and multiple sclerosis severely hamper the functioning of the CNS.[1] Psychiatric conditions including schizophrenia and clinical depression are also associated with brain dysfunctions.[2] Moreover, the incidence of cognitive impairment leads to behavioral changes, and eventually, under chronic conditions, it may develop into Alzheimer's disease (AD), which can prove fatal.[3] With ∼25 million people suffering from AD worldwide, the number is expected to double by 2050.[4] Since the disease is more prevalent in the aged population, increased life expectancy is also adding to the number of AD cases.[5] Despite the severe nature of this neurological disorder, there is no cure for the disease to date, while the current treatments for Alzheimer's disease merely address its symptoms. Even the reasons for the disease's origin are still not clearly known though complex molecular pathways including neurotransmitters,[6] oxidative stress,[7] nitrosative stress,[7] eicosanoids,[8] and inflammatory cytokine mediators[9] are expected to play key roles in the emergence of Alzheimer's disease.

While focusing on these biochemical pathways that contribute to the initiation and propagation of the disease, various treatment strategies targeting BACE-1,[10−15] AChE,[16−18] and kinases[19−21] are adopted to address AD. However, due to the multifactorial nature of this neuro-disorder, several single-target guided AD drugs did not pass through the clinical trials. It was, therefore, planned to develop new chemical entities that can target multiple AD-associated enzymes. We present here in vitro and in vivo experiments with a set of molecules against the AD-related cellular targets and identify some highly potent molecules.

Received: November 14, 2023
Revised: January 4, 2024
Accepted: January 11, 2024
Published: March 4, 2024

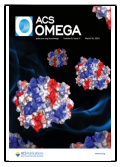

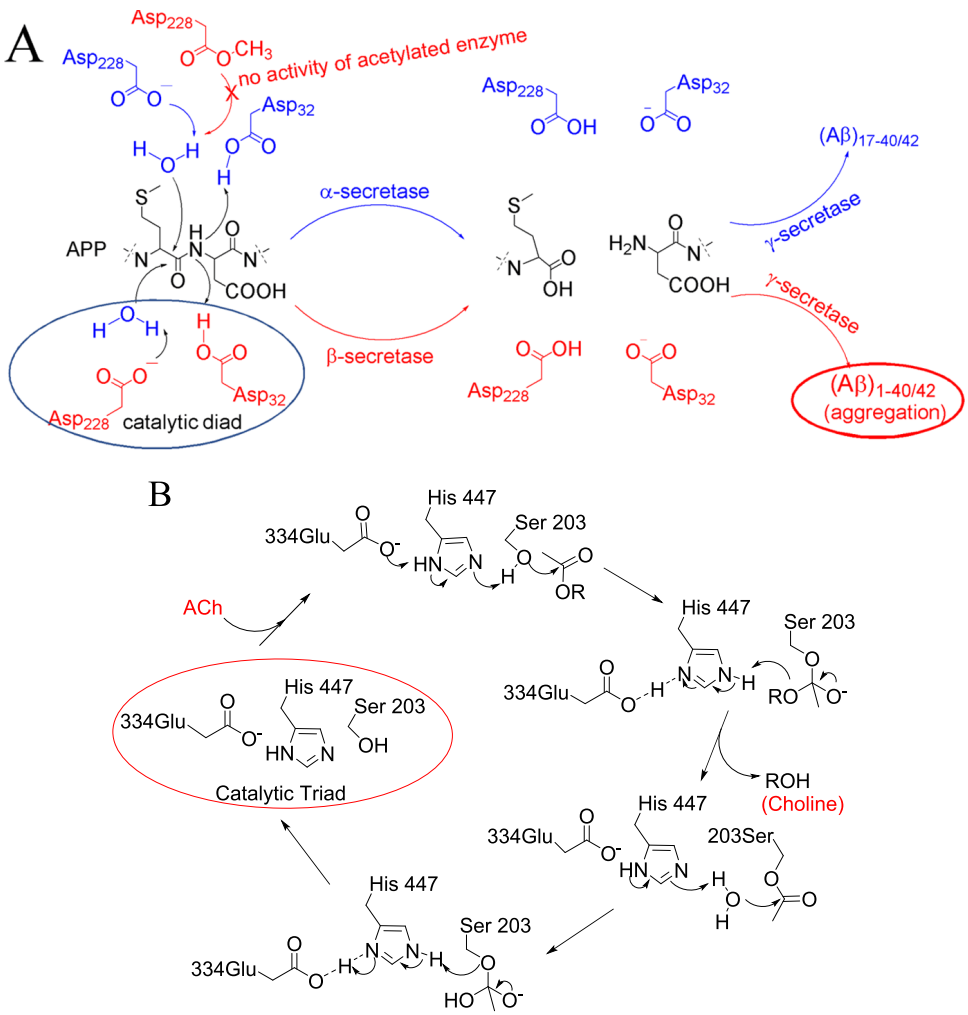

Figure 1. (A) Mechanism of APP breakdown (catalytic diad) under the effect of α-secretase (gray-blue part) and β-secretase (gray-red part). The action of β-secretase followed by γ-secretase is responsible for the generation of the amyloid β protein $(A\beta)_{1-40/42}$—the causative agent of AD. (B) Mechanism of AChE-mediated hydrolysis of ACh showing a catalytic triad.

2. RESULTS AND DISCUSSION

2.1. Selection of Targets and the Design Strategy for New Molecules. The most widely accepted pathologic reason for the appearance of AD symptoms is the accumulation of certain mass in the brain, which was later identified as amyloid β protein $(A\beta)_{1-40/42}$. This protein is formed by the action of BACE-1 on APP generating the soluble amyloid protein β (sAPPβ) and the subsequent action of γ-secretase on sAPPβ (red part, Figure 1).[22,23] It is observed that out of the two isoforms of β-secretase—the β-site APP cleaving enzyme 1 (BACE-1) and the β-site APP cleaving enzyme 2 (BACE-2)—present in the brain, BACE-1 plays a predominant role in the commencement of AD.[24] Mechanistically, the cleavage of APP at the Asp−Met juncture is accomplished by the participation of Asp32 and Asp228 (catalytic diad) of the active site of the enzyme (Figure 1A). The activation of an enzyme-bound water molecule by one of the two catalytic aspartates enables it to react at the carbonyl carbon of the amide group, thus releasing the products of peptide cleavage.[25] It is, therefore, inferred that the BACE-1 inhibitors must target the catalytic diad of the enzyme.

Another factor supplementing BACE-1 in the initiation/progression of AD is the reduced level of neurotransmitters, acetylcholine (ACh), in the brain. Since the ACh level is reduced due to the cholinesterase (AChE) activity, this enzyme served as the potential target of anti-AD drugs.[26] AChE-based hydrolysis of ACh is assisted by the Glu327, His440, and Ser200 triad (Figure 1B).[27] Apart from the active site, AChE contains a peripheral anionic site (PAS), which binds different kinds of ligands/uncompetitive inhibitors, thus changing the conformation of the active site and inhibiting the activity of AChE.[28] Hence, developing AChE inhibitors capable of interacting with its Glu327, His440, and Ser200 triad is one of the strategic approaches for the treatment of AD.

Therefore, keeping in view the two targets of AD-treatment agents, herein, the focus was on the design of dual inhibitors of BACE-1 and AChE. As per literature reports, structurally diverse BACE-1 and AChE inhibitors (Figure 2A)[29−34] consist of fused bicyclic systems such as indene, chromone, acridine, and indole, while pyrrolidine and piperidine also comprise an integral part of their structure. Since the active sites "diad" and "triad" of BACE-1 and AChE are constituted by polar residues, it was envisaged that the inhibitors of these enzymes must have an optimum log P and total polar surface area (TPSA) so that they can easily cross the BBB and interact in the active site pockets of the enzymes. Owing to the presence of polar groups in peptides and the possibility of their derivatization through N-/C- termini, it was planned to develop small peptides for

https://doi.org/10.1021/acsomega.3c09069
ACS Omega 2024, 9, 12896−12913

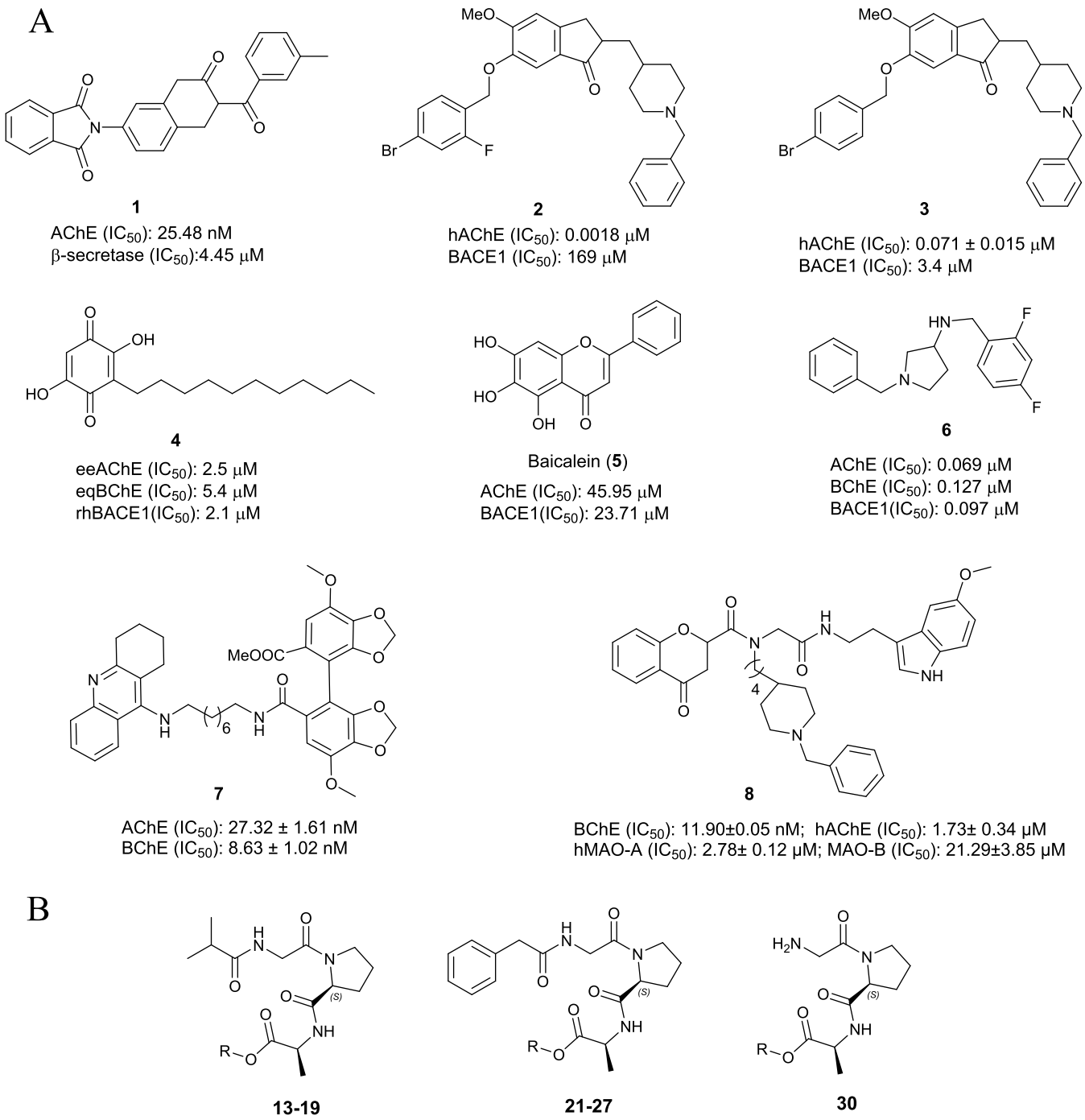

Figure 2. (A) Multitarget inhibitors of AD enzymes and (B) design of new molecules.

targeting BACE-1 and AChE. Moreover, for reducing the molecular flexibility and imparting a bent structure (controlled surface area), proline was chosen as the template, whereas hydrophobic moieties were tagged at the N-/C-termini to adjust the physicochemical properties of the molecules (Figure 2B).

Design of the molecules was validated by their molecular docking in the active site pockets of BACE-1 and AChE (Figures S1−S45 and Table S1). A number of H-bond and hydrophobic interactions between the molecules and the two enzymes were observed. Compound **27** interacts through the H-bond with G230 and D228 of BACE-1. It also makes two H-bonds with the water molecules in the active site (Figure 3A). Similarly, H-bonding of **25** with T76, R128, and water molecules was observed (Figure 3B). Appreciable interactions of the newly designed compounds were also observed in the active site pocket of AChE (Figure 3C,D). Both the compounds **15** and **25** were found to interact with H447 of the catalytic triad of AChE. Compound **25** orients in the active site of BACE-1 in a way that it interacts with T84 through its one arm and forms a H-bond with water molecules from its other end.

2.2. Chemistry. N-Boc protected L-proline **9** was coupled with L-Ala-OMe in the presence of triethylamine (TEA) and ethyl chloroformate (ECF) in tetrahydrofuran (THF) to procure compound **10**. The Boc group of **10** was removed with

https://doi.org/10.1021/acsomega.3c09069
ACS Omega 2024, 9, 12896−12913

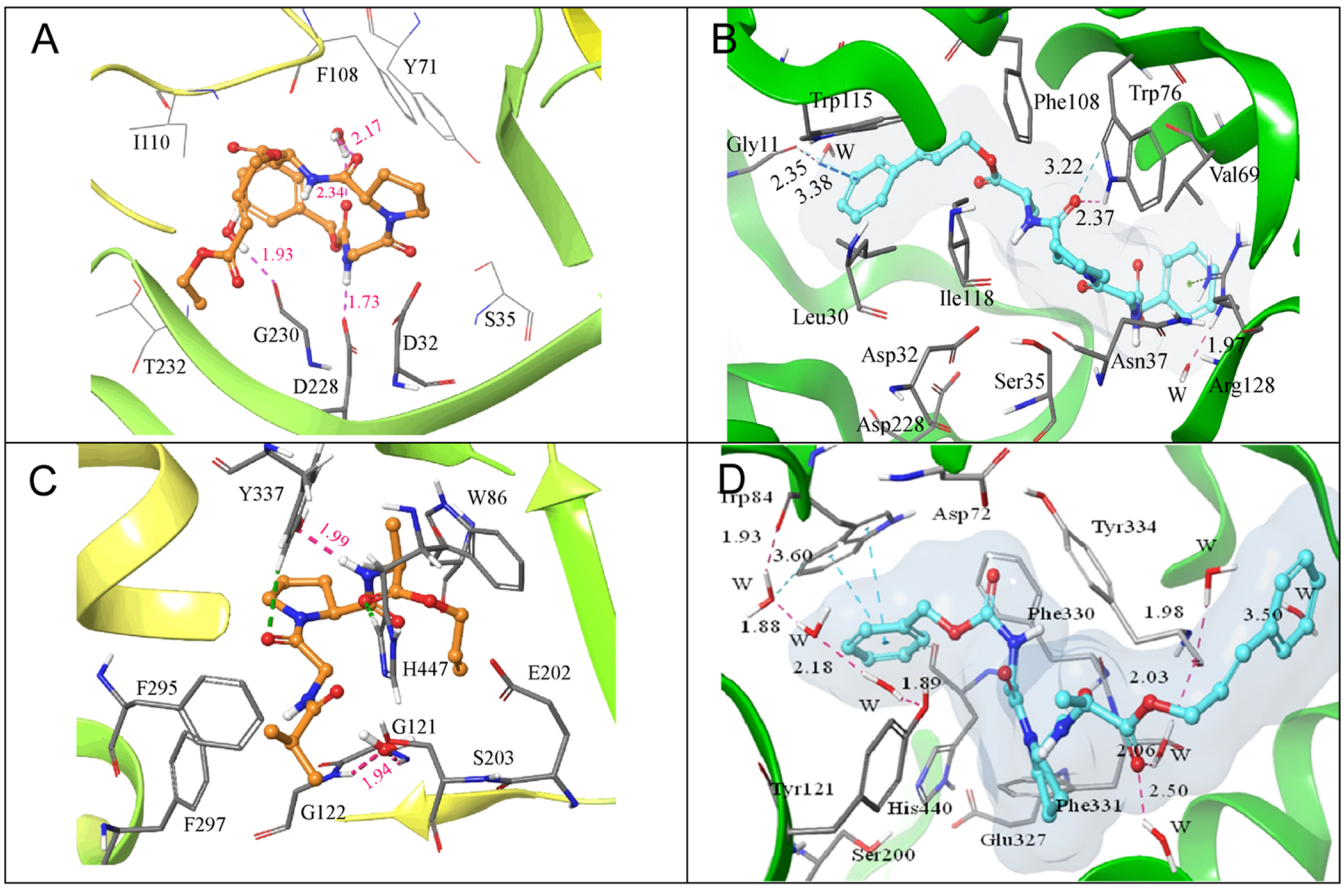

Figure 3. Binding mode of (A) Cbz-Gly-Pro-Ala-*O*-crotyl (**27**) in BACE-1 (PDB ID 6EQM),[35] (B) Cbz-Gly-Pro-Ala-*O*-cinnamyl (**25**) in BACE-1, (C) Iso-Gly-Pro-Ala-*O*-Allyl (**15**) in AChE, and (D) **25** in AChE (PDB ID 4EY6)[36] (also see the Supporting Information).

trifluoroacetic acid (TFA) to obtain compound **11**. Compound **12**, synthesized by the reaction of iso-butyric acid and Gly-OH, was coupled with **11** to get compound **13**. Compound **14**, obtained by the ester group hydrolysis of **13**, was re-esterified with allyl bromide/crotyl bromide/dimethyl bromide/propargyl bromide/geranyl bromide/cinnamyl bromide, and thereby compounds **15**−**19** were obtained (Scheme 1).

Further, Gly-OH was reacted with CbzCl, and the resulting compound **20** was coupled with **11** to get compound **21**. Ester hydrolysis of **21** gave compound **22**, which was derivatized with allyl/propargyl/crotyl/cinnamyl/geranyl/dimethylallyl bromides to obtain the series of compounds **23**−**27**. These esterifying agents and the isobut/Cbz groups helped in balancing the TPSA and logP of the compounds. For the synthesis of compound **30**, boc-Gly **28** was coupled with dipeptide **11** to get compound **29**, which was deprotected of the boc group to obtain **30** (Scheme 2). For comparison, due to providing more rigidity and hydrophobicity (less TPSA) to the molecule, compound **33** was included in the present studies. Synthesis of **33** was accomplished by the reaction of (*S*)-binol with propargyl bromide and the coupling of the resulting compound **31** with cinnamyl azide (Scheme 3).

2.3. Biological Studies. *2.3.1. BACE-1 Inhibitory Activities.* BACE-1 inhibitory activities of the compounds were determined by using bioassay kits. Among the compounds **13**−**19** (iso-butyric group at the N-terminal of the GPA tripeptide), the presence of allyl, dimethylallyl, and cinnamyl groups was best tolerated by BACE-1 as compounds **15**, **16**, and **17** exhibited IC_{50} values of 0.05, 0.2, and 0.1 μM, respectively (Table 1). In the case of compounds **21**−**27** (Cbz group at the N-terminal of GPA), compounds **25**, **26**, and **27** with cinnamyl, geranyl, and crotyl groups, respectively, at the O-terminus were found more potent. The IC_{50} values of compounds **25**, **27**, and **30** were similar to Calbiochem IV, which was employed as a control (IC_{50} 20 nM). In general, it was observed that the presence of the substituents at both the N- and O-termini of the GPA tripeptide influences the BACE-1 inhibitory activities of the compounds.

2.3.2. AChE Inhibitory Activities. All of the test compounds except for **15** were found to have IC_{50} values in the micromolar range. Compound **15** displayed an IC_{50} of 0.05 μM (Table 1), which was even better than the standard drug donepezil (IC_{50} 0.09 μM). A good correlation between the potency of the compounds and their extent of interactions with AChE was observed. The molecular docking of compound **15** (Figure 3) and its homologue **23** (Figure S10) in AChE showed that compound **23** is slightly displaced from the active site pocket. The higher IC_{50} of compound **16** in comparison to compound **15** may be attributed to its small number of interactions with the enzyme as was evident from the molecular docking studies. Compound **16** showed only one H-bond interaction with the water molecule present in the active site of the enzyme (Figure S4). Among the N-Cbz compounds **21**−**27**, compound **22** exhibited an IC_{50} value of 0.1 μM. The better activity of compound **22** also appeared due to its H-bond and π−π interactions with the amino acid residues of AChE (Figure S9). On the other hand, its methyl derivative **21** with IC_{50} in the millimolar range did not interact with any of the amino acids

https://doi.org/10.1021/acsomega.3c09069
ACS Omega 2024, 9, 12896−12913

Scheme 1. Syntheis of Compounds 15−27[a]

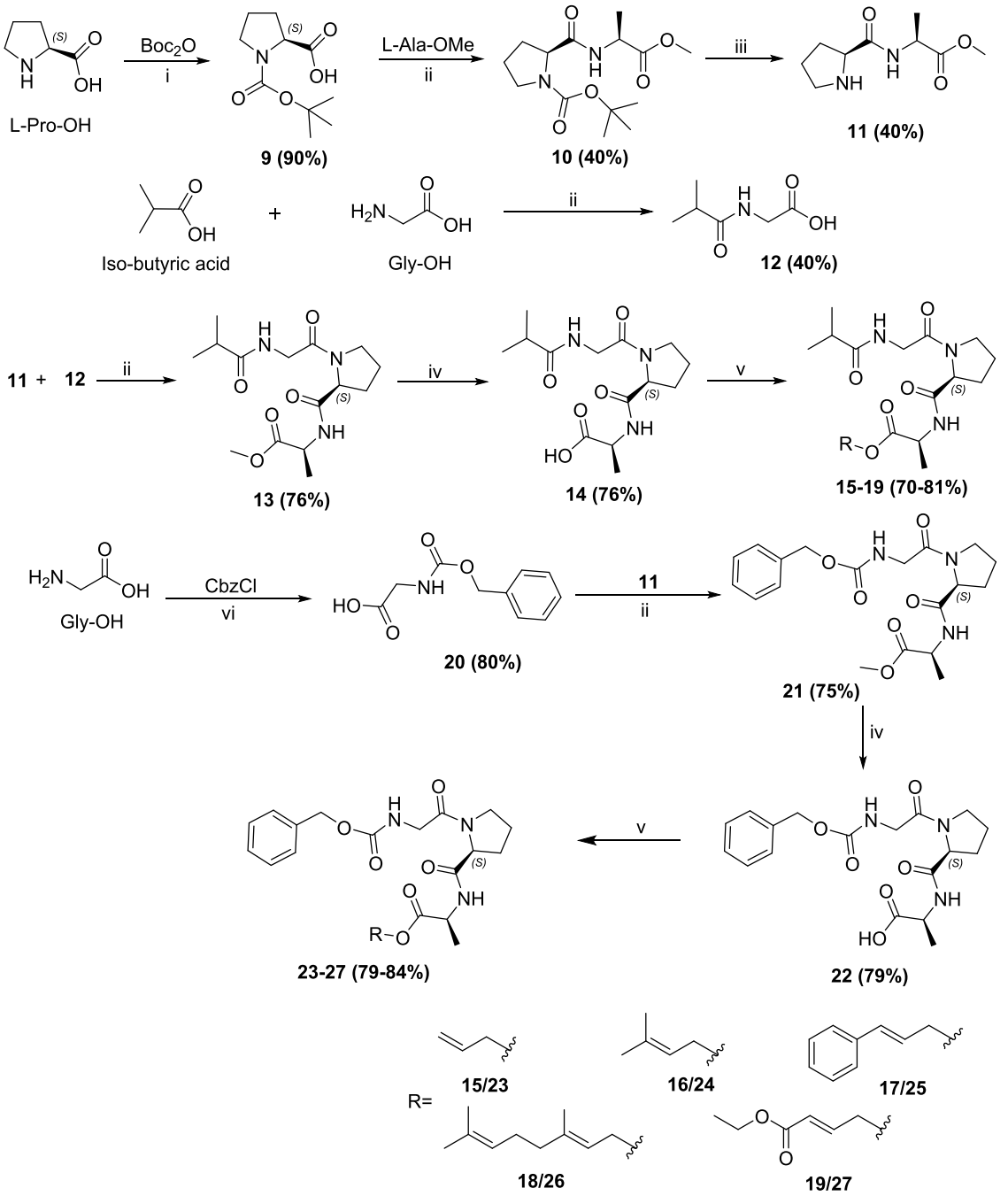

[a]Reaction conditions: (i) dioxane/H_2O (2:1), NaOH, rt,1.5 h; (ii) TEA, ECF, THF, −10 °C to rt, 8 h; (iii) TFA, DCM, 8 h; (iv) acetone/H_2O (3:2), NaOH, rt; (v) ACN, K_2CO_3, 60 °C, 12 h; (vi) CbzCl, NaOH, H_2O.

Scheme 2. Synthesis of Compounds 29 and 30[a]

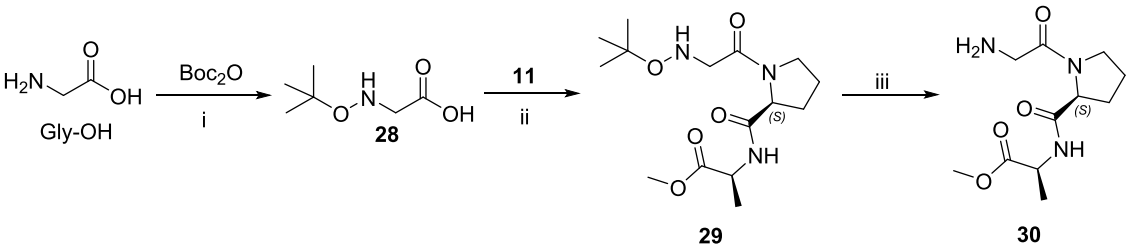

[a]Reaction conditions: (i) dioxane/H_2O (2:1), NaOH, rt,1.5 h; (ii) TEA, ECF, THF, −10 °C to rt, 8 h; (iii) TFA, DCM, 8 h.

https://doi.org/10.1021/acsomega.3c09069
ACS Omega 2024, 9, 12896−12913

Scheme 3. Synthesis of Compound 33[a]

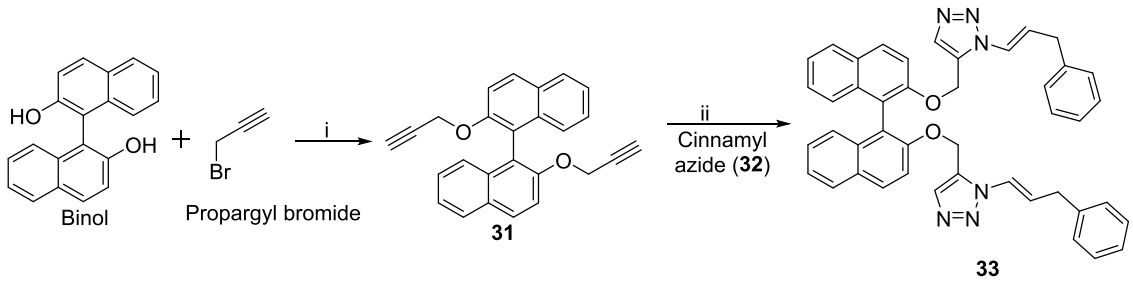

[a]Reaction conditions: (i) K_2CO_3, DMF, 60 °C; (ii) EtOH/H_2O (9:1), $CuSO_4 \cdot 5H_2O$, sodium ascorbate.

Table 1. BACE-1 and AChE Inhibitory Activities of Proline and Binol Derivatives

compound	structure	IC_{50} (μM) BACE-1	IC_{50} (μM) AChE	% inhibition of Aβ_{1-42} aggregation at 10 μM
13	isobut-GPA-OMe	0.2 ± 0.03	7 ± 1.0	36.3 ± 4.3
14	isobut-GPA−OH	0.6 ± 0.05	8 ± 1.2	
15	isobut-GPA-*O*-allyl	0.05 ± 0.001	0.05 ± 0.01	51 ± 6.1
16	isobut-GPA-*O*-dimethylallyl	0.2 ± 0.01	1 ± 0.1	
17	isobut-GPA-*O*-cinnamyl	0.1 ± 0.01	0.9 ± 0.1	
18	isobut-GPA-*O*-geranyl	20 ± 2.0	7 ± 1.3	12.48 ± 2.1
19	isobut-GPA-*O*-crotyl	30 ± 3.5	5 ± 1.1	
21	Cbz-GPA-OMe	30 ± 4.1	1000 ± 9.5	
22	Cbz-GPA−OH	0.3 ± 0.02	0.1 ± 0.01	
23	Cbz-GPA-*O*-allyl	1 ± 0.2	0.8 ± 0.1	
24	Cbz-GPA-*O*-dimethylallyl	20 ± 2.3	0.6 ± 0.03	
25	Cbz-GPA-*O*-cinnamyl	0.02 ± 0.001	1 ± 0.2	54.27 ± 8.4
26	Cbz-GPA-*O*-geranyl	0.1 ± 0.01	0.7 ± 0.1	31.79 ± 3.2
27	Cbz-GPA-*O*-crotyl	0.01 ± 0.001	1 ± 0.2	
30	NH_2-GPA-OMe	0.02 ± 0.001	2 ± 1.1	33.71 ± 4.2
33	binol-*O*-cinnamyl azole	1 ± 0.1	7 ± 1.4	43.22 ± 4.7
	donepezil		0.09 ± 0.01	10.95 ± 1.4
	calbiochem	0.02 ± 0.001		

present in the active site of AChE. Compounds **13** and **14** showed IC_{50} values in the micromolar range, and they were found to exhibit a H-bond interaction with water and $\pi-\pi$ stacking with H447, respectively (Figures S1 and S2). Derivatization of the free acid functionality of compound **14** with crotyl, geranyl, cinnamyl, dimethyl, and allyl substituents resulted in better IC_{50} values, whereas derivatization of **22** with these substituents increased the inhibitory concentrations of the compounds. In accordance with the results of molecular docking studies, the benzyl derivative **27** showed better inhibitory activity in comparison to compound **19**. Compound **33** also exhibited activity against BACE-1 and AChE although the presence of the binol moiety did not appear, providing a major additional advantage to the molecules.

2.3.3. Inhibition of Aβ_{1-42} Aggregation. Irrespective of the influence of metal ions, AChE, and oxidative stress, the aggregation of Aβ is unclear; here, the compounds **13**, **15**, **18**, **25**, **26**, **27**, **30**, and **33** were investigated for their ability to inhibit Aβ_{1-42} aggregation. Compound **15**, the potent inhibitor of both AChE (IC_{50} 0.05 μM) and BACE-1 (IC_{50} 0.05 μM), was found to inhibit Aβ_{1-42} aggregation by 51%, while another potent compound **25** exhibited 54% inhibition of Aβ_{1-42} aggregation (Figure 4).

2.3.4. Bioavailability. Penetration through the biological membranes is a critical aspect of the CNS targeting drugs. Compounds **15**, **17**, **18**, **19**, **25**, **27**, **30**, and **33** were examined

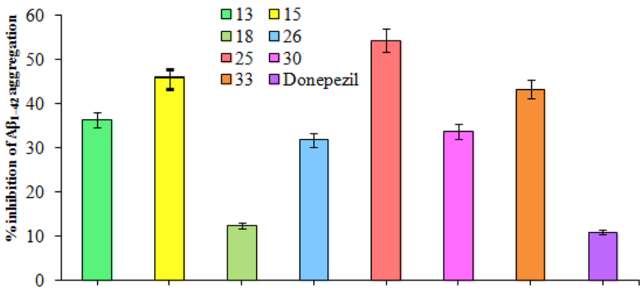

Figure 4. Percentage inhibition of Aβ_{1-42} aggregation at 10 μM exhibited by compounds **13**, **15**, **18**, **25**, **26**, **30**, and **33**.

for their ability to passively move in the parallel artificial membrane permeability experiment (Figure 5). Significant permeability of all of the compounds was observed with Pe values exceeding the breakpoint for permeable compounds given by PAMPA plate's manufacturer, i.e., Pe 1.5×10^{-6} cm s^{-1}. Generally, the CNS + compounds have Pe values $>4 \times 10^{-6}$ cm s^{-1}, while CNS- exhibit Pe $< 2 \times 10^{-6}$ cm s^{-1}. Pe values for compounds **19** and **25** were higher than the Pe values for the permeable compound caffeine (Pe = 10.9×10^{-6} cm s^{-1}) (Table 2).

2.3.5. In Vivo Studies on Mice Models. 2.3.5.1. Effect of Test Compounds on Latency Time: Time Taken by the Animal to Reach the Platform in the Morris Water Maze

https://doi.org/10.1021/acsomega.3c09069
ACS Omega 2024, 9, 12896−12913

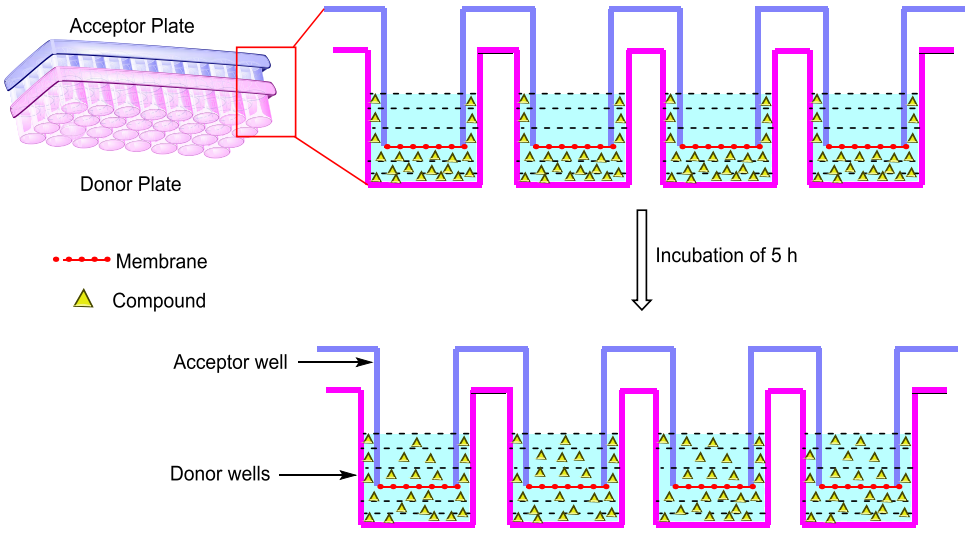

Figure 5. Pictorial representation of the two plates of the PAMPA system mimicking the BBB.

Table 2. Permeability Values (Pe) Calculated from the PAMPA-BBB Assay

compound	structure	Pe (cm s^{-1})
15	iso-GPA-*O*-allyl	$1.80 \pm 0.2 \times 10^{-6}$
17	iso-GPA-*O*-cinnamyl	$3.64 \pm 0.7 \times 10^{-6}$
18	iso-GPA-*O*-geranyl	$3.17 \pm 0.6 \times 10^{-6}$
19	iso-GPA-*O*-crotyl	$20.7 \pm 3.5 \times 10^{-6}$
25	Cbz-GPA-*O*-cinnamyl	$17.8 \pm 2.8 \times 10^{-6}$
27	Cbz-GPA-*O*-crotyl	$6.93 \pm 1.3 \times 10^{-6}$
30	NH_2-GPA-OMe	$8.98 \pm 2.1 \times 10^{-6}$
33	binol-*O*-cinnamyl azole	$1.59 \pm 0.3 \times 10^{-6}$
	caffeine[a]	$10.9 \pm 1.9 \times 10^{-6}$
	norfloxacin[b]	$1.73 \pm 0.2 \times 10^{-6}$

[a]Lit.:[37] 2.7×10^{-6} cm s^{-1}. [b]0.4×10^{-6} cm s^{-1} with lipid conc 100 mg mL^{-1}.

(MWM) Test. Animals were trained for 5 days so that they learn to reach the platform. The basal reading on the fifth day showed that all of the animals were trained adequately to be used in this study (Table 3). No significant difference in the latency time to reach the platform was observed in the different groups of animals (Figure 6). On the sixth day, the animal groups 3−8 were treated with donepezil (3 mg/kg), compound **30** (10 mg/kg), compound **15** (10 mg/kg), compound **18** (10 mg/kg), compound **25** (10 mg/kg), and compound **26** (10 mg/kg), respectively. On the 11th day (before scopolamine treatment), no significant difference in the time to reach the platform was observed in all of the animal groups except the animals of group 8 (compound **26** treated) (Figure 6A). Scopolamine treatment on the 12th, 13th, and 14th days increased the latency to reach the platform in comparison to the normal animals, thus indicating the memory-impairing effect of scopolamine (Table 3). Considerable reduction in the time taken by the animals in group 3 (donepezil-treated) to reach the platform was observed in comparison to the scopolamine-treated group 2 (Figure 6C). Noticeably, the pretreatment with the test molecules, compound **30** (10 mg/kg), compound **25** (10 mg/kg), and compound **26** (10 mg/kg) also alleviated the memory-impairing effect of scopolamine when a significant reduction in the latency time to reach the platform was observed in animal groups 4, 7, and 8. However, pretreatment with compounds **15** and **18** did not show a significant effect on scopolamine-induced memory impairment. Compound **15**, although highly potent in the in vitro experiments, had a poor effect on scopolamine-induced memory impairment, which may be attributed to its low permeability through the biological membrane. The effect of compound **25** was similar to that observed with the standard drug donepezil (Figure 6C and Table 4).

2.3.5.2. Effect of the Test Compounds on the Latency Time to Reach the Shock-Free Area in the Passive Avoidance Task (PAT). As observed in the MWM test, no significant difference in the latency time to reach the shock-free area was seen in the PAT test after the standard and the test treatments (until the 11th day, before scopolamine treatment) (Figure 7A). Scopolamine treatment for the three consecutive days (12th, 13th, and 14th days) significantly increased the latency time, indicating its memory-impairing effect. Pretreatment with donepezil (3 mg/kg) reduced the latency to reach the shock-free area in a short while as compared to the scopolamine-treated group. Similar to donepezil, pretreatment with compound **30** (10 mg/kg), compound **18** (10 mg/kg), compound **25** (10 mg/kg), and compound **26** (10 mg/kg) also improved the memory-impairing effect of scopolamine. However, pretreatment with compound **15** did not have a significant effect on scopolamine-induced memory impairment in the PAT test too (Figure 7B).

2.3.6. Lipinski Parameters and ADME Profile. Drug likeness properties such as Lipinski parameters (Table 5) and the ADME profile (Table S2) of the test compounds were checked and correlated with the results of biological studies. Molecular weight of all of the compounds is <500 Da except for compound **33**. It has been proposed that compounds with high lipophilicity ($c \log P > 3$) are likely to have a higher chance of toxicity in animal studies in comparison to compounds with lower lipophilicity ($c \log P < 3$).[38] Most of the compounds were found to exhibit $c \log P < 3$ except for compounds **18**, **26**, **32**, and **33**. Since donepezil was found to be extensively metabolized by CYP 2D6 and CYP 3A4 isoforms of CYP 450, we also estimated the possibility of metabolism of the designed compounds with these two isoforms using PreADME software. Only compound **30** was

https://doi.org/10.1021/acsomega.3c09069
ACS Omega 2024, 9, 12896−12913

Table 3. Starting from the Blue Dot, Trajectory Plots of Each Animal from the Different Groups

Groups	Day 1	Day 5	Day 11	Day 14
Normal	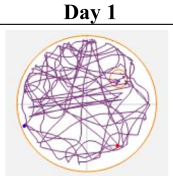	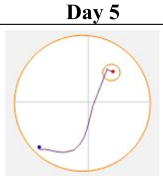	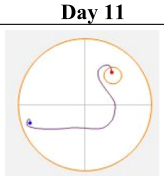	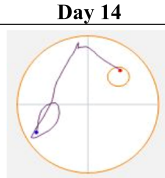
Scopolamine	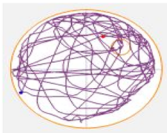	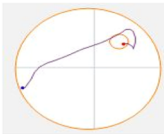	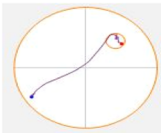	
Donepezil		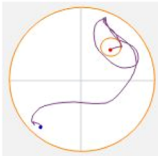	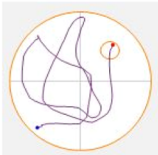	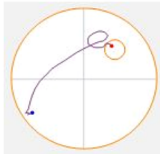
30	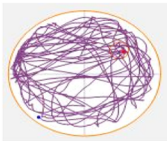		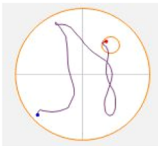	
15		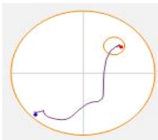	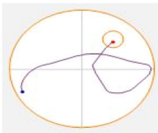	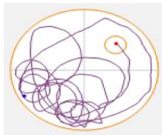
18	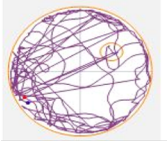	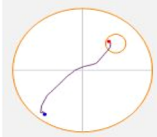	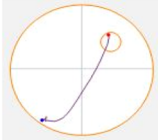	
25		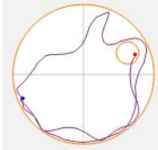	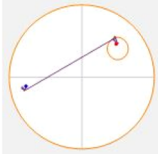	
26	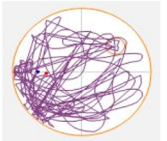	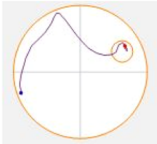	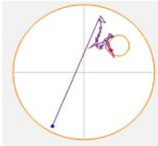	

found to be a weak substrate of CYP 2D6 among the series (Table S2). Compounds **12**, **13**, **19**, and **21**−**29** appeared as the substrates of CYP 3A4, whereas the binol derivatives (compounds **33**, **32**) displayed an enzyme inhibition effect. When given orally, a compound with higher human intestinal absorption (HIA) is more likely to be absorbed from the intestinal tract. Except for compound **31**, all of the other compounds had HIA > 50. Plasma protein binding can also enhance the solubility of the molecules, especially the hydrophobic ones, as well as it protects the drugs from oxidation, reduces toxicity, and extends their half-life. All of the compounds were found to have good plasma binding capacity.

2.3.7. Plasma Stability Assay. Compound **25** was checked for its stability through a plasma stability assay.[39] A solution of compound **25** in PBS (50 μM) was used as the positive control. Compound **25** was taken in plasma (pH 7−8) to produce the solution of final concentration 50 μM. After incubation of the sample at 37 °C for 1 h and 12 h, 400 μL of acetonitrile was added to quench the reaction. The concentration of the compound in plasma was quantified from the HRMS chromatograms of the treated supernatant and buffer solutions. The percentage of analyte lysed by plasma of each solution was calculated from intensities of peaks observed in the HRMS spectra at the same interval of time using eq 1.

$$\%\ \text{of analyte lysed by plasma} = \frac{I_0 - I}{I_0} \times 100 \quad (1)$$

where I_0 and I represent the intensities of compounds in the presence of buffer and plasma (treated supernatant), respectively. Remarkably, a slight change in the concentration of **25** (∼10%) was observed after 12 h of incubation (Figures S137−S139). It is demonstrated that plasma had no

https://doi.org/10.1021/acsomega.3c09069
ACS Omega 2024, 9, 12896−12913

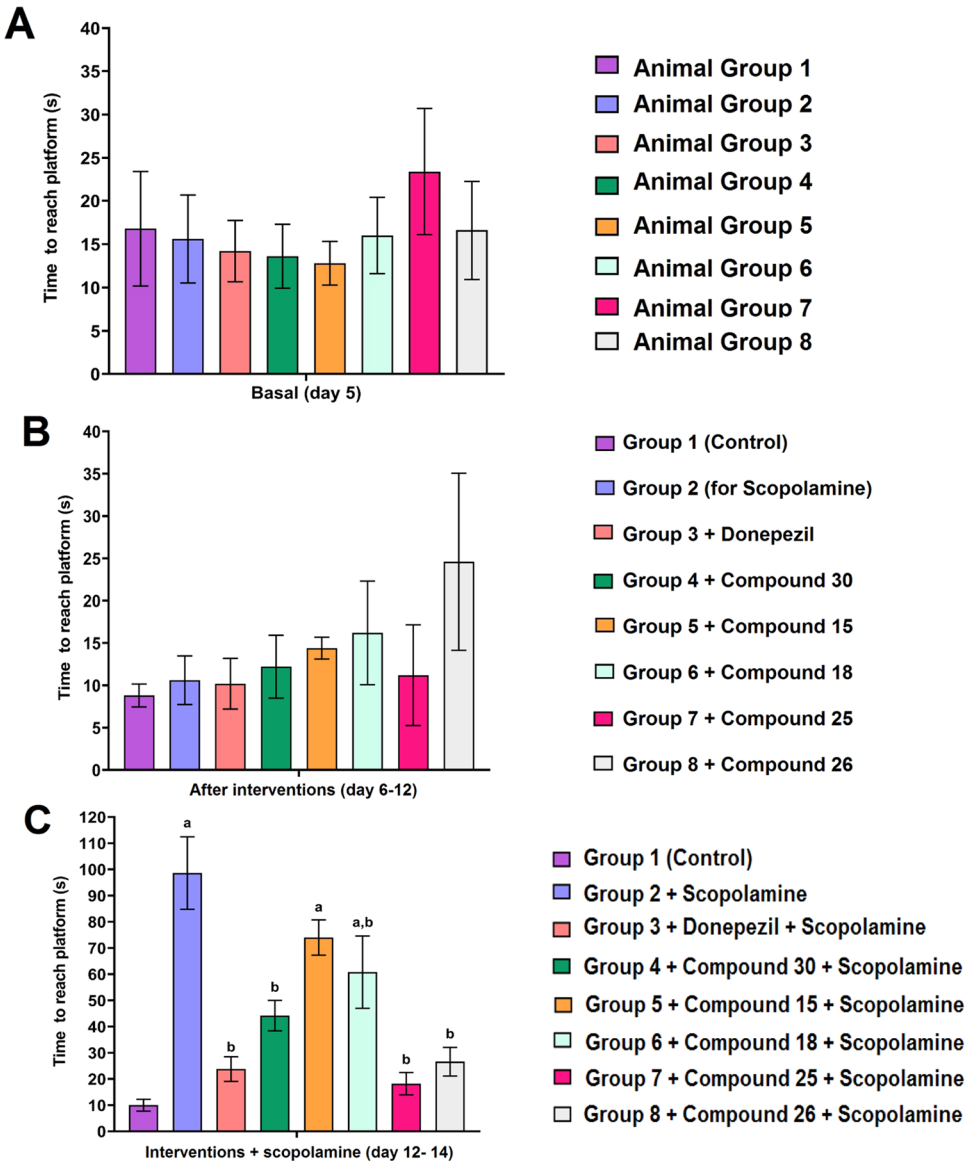

Figure 6. (A) Basal reading on day 5 after 4 days of training and before the start of the test treatment in MWM. (B) Effect of various compounds (10 mg/kg) on the animals' memory before scopolamine treatment. (C) Effect of the compounds (10 mg/kg) on the animals' memory after inducing impaired memory with scopolamine. Data were analyzed by using a one-way analysis of variance followed by Tukey's test ($^{a}p < 0.05$ vs the control group, $^{b}p < 0.05$ vs scopolamine).

Table 4. Reversal of Scopolamine-Induced Memory Impairment in the Presence of the Test Compound. This Data Corresponds to One Animal from Each Group

	time (in s) taken by the animals to reach the platform		
groups	after the training (5th day)	after treatment with the test compound/donepezil (11th day)	after treatment with scopolamine (14th day)
control	6	6	10
scopolamine	8	3	77
donepezil	15	17	10
15	11	11	93
18	5	5	71
25	20	15	15
26	7	39	45
30	20	12	65

remarkable effect on the half-life time of **25**, and further, it can be prioritized for in vivo studies.

3. CONCLUSIONS AND REMARKS

The compounds designed after analyzing the catalytic modes of BACE-1 and AChE proved highly effective against the Alzheimer's disease animal models. The functioning of the catalytic processes of these two enzymes through the participation of a polar diad consisting of Asp228 and Asp32 for BACE-1 and the triad of Glu334, His447, and Ser203 for AChE laid the basis for the design of new molecules having a higher total polar surface area (TPSA) than the reported compounds (**1**−**8**, Table 5) so that they better interact in the catalytic pocket of the enzymes. The derivatization of the Gly−Pro−Ala tripeptide through its N- and O-termini was appropriately achieved in making the required hydrophobic−hydrophilic balance in the molecule (logP and TPSA). In comparison to compounds **1**−**8** in Table 5, compound **25** has

https://doi.org/10.1021/acsomega.3c09069
ACS Omega 2024, 9, 12896−12913

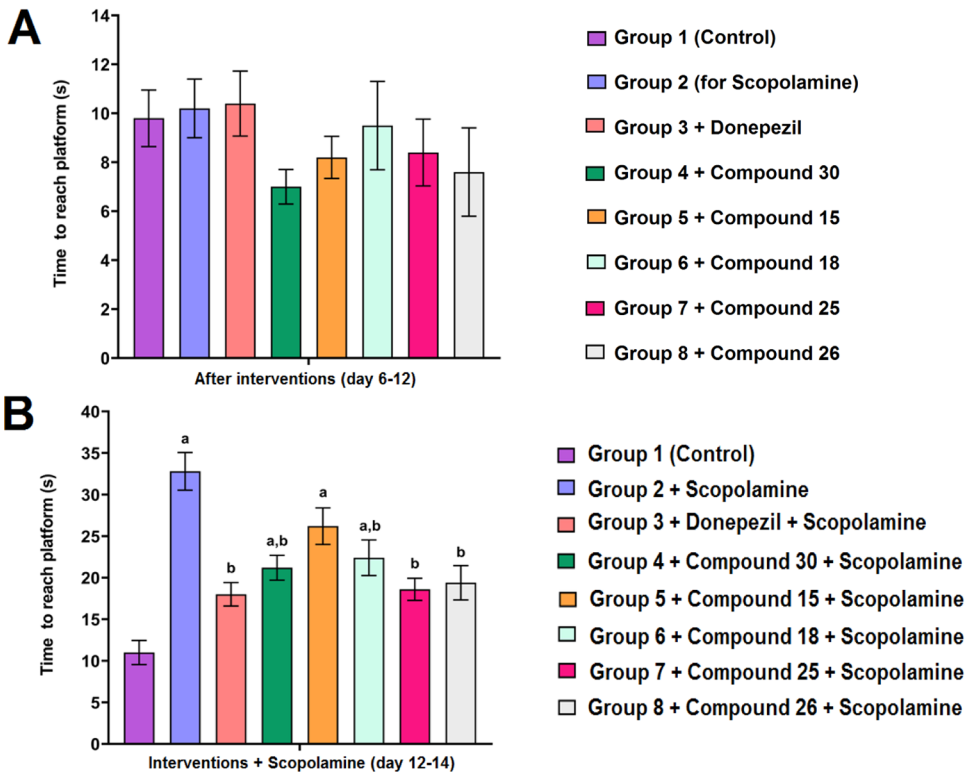

Figure 7. PAT assay: effect of the compounds (10 mg/kg) on memory in PAT (A) before scopolamine treatment and (B) after treatment with scopolamine to induce impaired memory in PAT. Data were analyzed by using a one-way analysis of variance followed by Tukey's test ($^a p < 0.05$ vs the control group, $^b p < 0.05$ vs scopolamine).

log *P* 2.61 and TPSA 104. The in vitro and in vivo screening of the molecules led to the identification of highly potent molecules. While appreciably potent in the enzyme immunoassays, compound **25** exhibited the best biological membrane permeability, and it was identified as the most effective in reversing scopolamine-induced memory impairment in mice models. It implies that a suitable combination of log *P* and TPSA is desirable for the better biological activity of the molecule. In accordance with the reported observations, it was noticed that a compound with considerable in vitro potency may not be effective under the in vivo conditions; such a case was represented by compound **15**. Therefore, adopting a rational approach of drug designing, the integration of in silico and wet-lab experiments resulted in the identification of some highly potent molecules, which can be taken to the next level of investigations.

4. EXPERIMENTAL SECTION

4.1. General. All of the solvents were of chromatography grade and used without further purification. The chemicals were purchased either from Sigma-Aldrich or from S.d. fine/Spectrochem. Thin-layer chromatography (TLC) was performed using silica plates precoated with silica gel GF-254 (Qualigens, India). Column chromatography was performed with a silica 60−120 mesh. LC-MS and high-resolution mass spectra were recorded on a Bruker micrOTOF-QII mass spectrometer using the +ve/−ve ion mode. Melting points were determined in capillaries. ^{1}H and ^{13}C NMR spectra were recorded in $CDCl_3$ and/or DMSO-d_6 on a Bruker 500 and 125 MHz NMR spectrometer, respectively. Chemical shifts are given in ppm with TMS as an internal reference. Coupling constants (*J*) are given in Hz. Signals are abbreviated as singlet, s; doublet, d; double−doublet, dd; triplet, t; and multiplet, m. In ^{13}C/DEPT-135 data, the +ve sign corresponds to signals due to CH_3 and CH groups, while the −ve sign symbolizes signals of CH_2 groups, and signals of quaternary carbon are absent (ab) in the DEPT-135 spectra. IR and UV−vis spectral data were recorded on FTIR Agilent CARY 630 and BIOTEK Synergy H1 Hybrid Reader instruments, respectively. Scopolamine was purchased from Sovereign Pharma Pvt. Ltd., India. Donepezil was purchased from Sigma-Aldrich. Percentage purity of the compounds was checked with q^{1}H NMR spectra.[40]

4.2. General Synthetic Procedure. *4.2.1. Procedure A.* A suspension of L-amino acid (0.01 mol) in 10 mL of dioxane/water (2:1) was dissolved in 0.01 mol sodium hydroxide at room temperature (1 M). After stirring the reaction mixture for 5 min at room temperature, 0.01 mol of Boc_2O was added and continuously stirred for 1.5 h. The dioxane was then vacuum-evaporated, and the aqueous portion was acidified to pH 2 using dil HCl. To obtain the required N-Boc-AA−OH, the released oil was extracted with ethyl acetate, dried over anhydrous sodium sulfate, and concentrated under vacuum.

4.2.2. Procedure B. L-Amino acid (0.01 mol) was dissolved in 4 M sodium hydroxide solution (0.01 mol) and chilled to 0 °C. Over 30 min, 0.01 mol of benzyl chloroformate and 0.01 mol of 4 M sodium hydroxide solution were added alternatively and portion-wise while stirring at 0 °C. The reaction mixture was then allowed to stir for 1 h at room temperature. The reaction mixture's contents were rinsed with 2 × 15 mL of ether, acidified with dil HCl to pH 2, extracted with ether, dried over anhydrous sodium sulfate, and concentrated in vacuum.

https://doi.org/10.1021/acsomega.3c09069
ACS Omega 2024, 9, 12896−12913

Table 5. Lipinski Parameters of the Compounds[a]

compound	mi log P	TPSA (Å^2)	MW (g/mol)	nON	nOHNH
1	4.27	73.22	409.44	5	0
2	6.60	38.78	552.48	4	0
3	6.50	38.78	534.49	4	0
4	4.62	74.60	294.39	4	2
5	2.68	90.89	270.24	5	3
6	3.30	15.27	302.37	2	1
7	5.35	135.73	641.68	12	2
8	4.74	103.97	608.74	9	2
13	−0.42	104.81	327.38	8	2
14	−2.49	115.80	313.25	8	3
20	−0.44	66.40	193.20	4	2
21	0.26	104.81	375.43	8	2
22	−1.81	115.80	361.40	8	3
15	0.23	104.81	353.42	8	2
16	1.26	104.81	381.47	8	2
17	1.93	104.81	429.52	8	2
18	3.10	104.81	449.59	8	2
19	0.34	131.12	425.48	10	2
23	0.91	104.81	401.46	8	2
24	1.94	104.81	429.52	8	2
25	2.61	104.81	477.56	8	2
26	3.78	104.81	497.64	8	2
27	1.02	131.12	473.53	10	2
28	−0.42	58.56	147.17	4	2
29	0.28	96.97	329.40	8	2
30	−1.84	101.73	257.29	7	3
32	6.39	18.47	362.43	2	0
33	8.93	79.90	680.81	8	0

[a]**1**−**8**: Reported compounds (Figure 2A); **9**−**33**: compounds of present investigations.

4.2.3. Procedure C. Triethylamine (0.021 mol) was added to a solution of N-Boc-AA (N-Boc-amino acid) (1 mmol) in THF (50 mL) at −10 °C followed by the addition of ethyl chloroformate (0.014 mol). To this reaction mixture, neutralized AA methyl ester hydrochloride (1.2 mmol) in 5 mL of THF was added at −10 °C. The reaction mixture was stirred at 0 °C to −10 °C for 1 h and then shifted to stir at 25 ± 2 °C for 12 h. After completion of the reaction, THF was evaporated under vacuum. The residue was then dissolved in 100 mL of ethyl acetate and washed with water (30 mL). The organic layer was washed with 5% Na_2CO_3 solution and 5% citric acid solution, dried over anhydrous Na_2SO_4, and evaporated to dryness under vacuum. The crude product was purified with column chromatography using ethyl acetate:hexane as the eluent to yield pure N-Boc-AA-AA methyl ester.

4.2.4. Procedure D. A solution of N-Boc-AA-AA methyl ester (0.01 mol) in acetone−water (3:2) was progressively added to 1 N NaOH (0.01 mol) at 25 ± 2 °C. The reaction mixture was stirred for 1 h. After the reaction was complete, acetone was evaporated under vacuum. The remaining part of the reaction mixture was acidified with dil HCl, and the product was extracted with ethyl acetate.

4.2.5. Procedure E. N-Boc-AA-AA(OMe) in dichloromethane (DCM) was added to a solution of trifluoroacetic acid (10 equiv of the peptide) and stirred at room temperature for 8 h. After completion of the reaction (TLC), the reaction mixture was concentrated in vacuum followed by washing with diethyl ether (3 × 10 mL) to obtain the desired product.

4.2.6. Procedure F. To the solution of AA−OH (1 mmol) in ACN at 60 °C, K_2CO_3 (1.5 mmol) was added, followed by the addition of allyl bromide/dimethyl bromide/crotyl bromide/cinnamyl bromide/geranyl bromide (1.2 mmol). The reaction was stirred at 60 °C for 12 h. After quenching the reaction mixture with ice, the crude product was extracted with ethyl acetate, followed by washing with water (30 mL). After drying over anhydrous sodium sulfate, the excess solvent was evaporated under vacuum to get the desired compound.

4.2.7. Procedure G. (*S*)-BINOL (1 mmol) in acetone was taken in a round-bottom flask fixed with a reflux condenser. To this solution, anhydrous potassium carbonate (3 mmol) was added, followed by the addition of propargyl bromide (3 mmol). The reaction mixture was allowed to stir for 16 h at 60 °C. The reaction mixture was evaporated on a rotary evaporator. The residue was purified by recrystallization (ethyl acetate/diethyl ether) to give compound **31** in 95% yield.

4.2.8. Procedure H. To the solution of cinnamyl bromide (1 mmol) in DMF, sodium azide (3 mmol) was added. The reaction mixture was allowed to stir at 60 °C for 2 h. After the completion of reaction, it was quenched with water and extracted with ethyl acetate. Then, the ethyl acetate layer was passed through Na_2SO_4 and the solvent was evaporated on a rotary evaporator to get the compound as a pale-yellow liquid.

4.2.9. Procedure I. To the solution of compound **31** (0.35 mmol) in ethanol (7 mL), sodium ascorbate (0.01 mmol) and $CuSO_4.5H_2O$ (0.03 mmol) were added. Further, a solution of cinnamyl azide (1.78 mmol) in ethanol was added to it. The reaction mixture was allowed to stir at room temperature for 12 h. After completion of the reaction (TLC), the reaction mixture was extracted with ethyl acetate. Ethyl acetate was then evaporated on a rotary evaporator to get a thick oil as the desired product.

*4.2.10. Boc-Pro-OH (**9**).* Compound **9** was synthesized according to the general procedure A as a colorless liquid; yield 90%; HRMS (microTOF-QII, MS, ESI): calcd for $C_{10}H_{17}O_3N$ ([M + H]$^+$) 222.1100, found 222.1103.

*4.2.11. Boc-Pro-Ala-OMe (**10**).* Compound **10** was synthesized according to the general procedure C as a colorless liquid; yield 40%; ^{1}H NMR (500 MHz, $CDCl_3$, 25 °C, TMS): δ 1.40 (d, J = 6.56 Hz, 3H, CH_{3Ala}), 1.48 (s, 9H, CH_{3Boc}), 1.84−2.02 (m, 2H, CH_{2Pro}), 2.05−2.32 (m, 2H, CH_{2Pro}), 3.36−3.50 (m, 2H, CH_{2Pro}), 3.75 (s, 3H, OCH_3), 4.08−4.31 (m, 1H, CH_{Ala}), 4.49−4.64 (m, 1H, CH_{Pro}), 7.28 (br, 1H, NH); HRMS (microTOF-QII, MS, ESI): calcd for $C_{14}H_{24}O_5N_2$ ([M + Na]$^+$) 323.1577, found 323.1579.

*4.2.12. NH-Pro-Ala-OMe (**11**).* Compound **11** was synthesized using the general procedure E as a colorless liquid; yield 40%; ^{1}H NMR (500 MHz, $CDCl_3$, 25 °C, TMS): δ 1.33 (d, J = 6.56 Hz, 3H, CH_{3Ala}), 1.76−1.99 (m, 3H, CH_{2Pro}), 2.31−2.34 (m, 1H, CH_{2Pro}), 3.20−3.24 (m, 2H, CH_{2Pro}), 3.64 (s, 3H, OCH_3), 4.24−4.25 (m, 1H, CH_{Ala}), 4.32−4.35 (m, 1H, CH_{Pro}), 8.88 (d, J = 6.88 Hz, 1H, NH), 9.02 (d, J = 6.18 Hz, 1H, NH); HRMS (microTOF-QII, MS, ESI): calcd for $C_9H_{16}O_3N_2$ ([M + H]$^+$) 201.1233, found 201.1282.

*4.2.13. Isobut-Gly-OH (**12**).* Compound **12** was synthesized according to the general procedure D as a colorless liquid; yield 40%, mp 107 °C; ^{1}H NMR (500 MHz, DMSO-d_6, 25 °C, TMS): δ 1.01 (d, J = 7.08 Hz, 6H, CH_3), 2.39−2.44 (m, 1H, CH), 3.71 (d, J = 6.03 Hz, 2H, CH_{2Gly}), 8.06 (t, J = 5.58 Hz, 1H, CH_{NH}), 12.45 (br, 1H, OH); ^{13}C NMR (125 MHz, normal/DEPT-135): δ 19.88 (+ve, CH_3), 34.18 (+ve, CH),

https://doi.org/10.1021/acsomega.3c09069
ACS Omega 2024, 9, 12896−12913

40.90 (−ve, CH_2), 43.46 (−ve, CH_{2Gly}), 171.95 (C═O), 176.94 (C═O); HRMS (microTOF-QII, MS, ESI): calcd for $C_6H_{11}O_3N$ ([M + Na]$^+$) 168.0631, found 168.0657.

*4.2.14. Isobut-Gly-Pro-Ala-OMe (**13**).* Compound **13** was synthesized according to the general procedure C as a white solid, yield 76%, mp 172 °C; $[\alpha]_D^{25}$ −105° (0.4, $CHCl_3$); IR (ATR): 3257, 3086, 2959, 2363, 1729, 1640, 1558, 1453, 1237, 1051, 998, 924, 775, 685 cm^{-1}; ^{1}H NMR (500 MHz, $CDCl_3$, 25 °C, TMS): δ 1.17 (d, J = 6.97 Hz, 6H, 2 x CH_{Iso}), 1.40 (t, 3H, J = 7.13 Hz, CH_{3Ala}), 1.94−2.04 (m, 2H, CH_{2Pro}), 2.12−2.17 (m, 1H, CH_{2Pro}), 2.29−2.34 (m, 1H, CH_{2Pro}), 2.42−2.50 (m, 1H, CH_{Iso}), 3.45 (q, J = 9.70 Hz, 1H, CH), 3.56−3.61 (m, 1H, CH_{2Pro}), 3.74 (s, 3H, OCH_3), 3.97−4.01 (m, 1H, CH), 4.09−4.13 (m, 1H, CH), 4.48−4.55 (m, 2H, OCH_2), 6.51 (br, 1H, NH), 7.04 (d, J = 6.94 Hz, 1H, NH); ^{13}C NMR (125 MHz, normal/DEPT-135): δ 18.07 (+ve, CH_3), 19.49 (+ve, CH_3), 19.55 (+ve, CH_3), 24.79 (−ve, CH_{2Pro}), 27.95 (−ve, CH_{2Pro}), 35.36 (+ve, CH), 42.01 (−ve, CH_{2Gly}), 46.47 (−ve, CH_{2Pro}), 48.24 (+ve, CH_{Ala}), 52.46 (+ve, CH_{Pro}), 60.14 (−ve, CH_2), 168.30 (C═O), 170.49 (C═O), 172.29 (C═O), 177.11 (C═O); HRMS (microTOF-QII, MS, ESI): calcd for $C_{15}H_{25}O_5N_3$ ([M + Na]$^+$) 350.1686, found 350.1674.

*4.2.15. Isobut-Gly-Pro-Ala-OH (**14**).* Compound **14** was synthesized according to the general procedure D as a white solid, yield 76%, mp 184 °C; $[\alpha]_D^{25}$ −102.5° (0.4, $CHCl_3$); IR (ATR): 3295, 3220, 3071, 2974, 2363, 1729, 1640, 1550, 1453, 1222, 1148, 1058, 924, 857, 775 cm^{-1}; ^{1}H NMR (500 MHz, DMSO-d_6, 25 °C, TMS): δ 1.00 (d, J = 6.76 Hz, 6H, 2 x CH_{Iso}), 1.27 (m, 3H, J = 7.13 Hz, CH_{3Ala}), 1.75−1.78 (m, 1H, CH_{2Pro}), 1.83−1.91 (m, 2H, CH_{2Pro}), 1.97−2.04 (m, 1H, CH_{2Pro}), 2.43−2.48 (m, 1H, CH_{Iso}), 3.43−3.48 (m, 1H, CH_{2Pro}), 3.50−3.55 (m, 1H, CH_{2Pro}), 3.75−3.79 (m, 1H, CH_{2Gly}), 3.93−3.97 (m, 1H, CH_{2Gly}), 4.11−4.17 (m, 1H, CH), 4.33−4.35 (m, 1H, CH), 7.82−7.86 (m, 1H, NH), 6.51 (br, 1H, NH), 8.18 (d, J = 7.36 Hz, 1H, NH), 12.56 (br, 1H, OH); ^{13}C NMR (125 MHz, normal/DEPT-135): δ 17.50 (+ve, CH_3), 19.98 (+ve, CH_3), 20.03 (+ve, CH_3), 24.61 (−ve, CH_{2Pro}), 29.49 (−ve, CH_{2Pro}), 34.14 (+ve, CH), 41.43 (−ve, CH_{2Gly}), 46.28 (−ve, CH_{2Pro}), 47.85 (+ve, CH_{Ala}), 48.04 (+ve, CH_{Pro}), 59.55 (−ve, CH_2), 167.52 (C═O), 171.87 (C═O), 174.51 (C═O), 176.74 (C═O); HRMS (microTOF-QII, MS, ESI): calcd for $C_{14}H_{23}O_5N_3$ ([M + K]$^+$) 352.1265, found 352.1269.

*4.2.16. Isobut-Gly-Pro-Ala-O-allyl (**15**).* Compound **15** was synthesized according to the general procedure F as a white solid, yield 70%, mp 150 °C; $[\alpha]_D^{25}$ −40° (0.4, $CHCl_3$); IR (ATR): 3257, 3086, 2974, 2087, 1744, 1640, 1558, 1453, 1326, 1200, 158, 924, 693, 625, 603 cm^{-1}; ^{1}H NMR (500 MHz, $CDCl_3$, 25 °C, TMS): δ 1.17 (d, J = 6.94 Hz, 6H, 2 x CH_{Iso}), 1.42 (t, 3H, J = 7.03 Hz, CH_{3Ala}), 1.92−2.04 (m, 2H, CH_{2Pro}), 2.11−2.19 (m, 1H, CH_{2Pro}), 2.30−2.34 (m, 1H, CH_{2Pro}), 2.41−2.48 (m, 1H, CH_{Iso}), 3.45 (q, J = 9.72 Hz, 1H, CH), 3.56−3.60 (m, 1H, CH_{2Pro}), 3.97−4.01 (m, 1H, CH), 4.07−4.13 (m, 1H, CH), 4.50−4.56 (m, 2H, CH_2), 4.61−4.66 (m, 2H, CH_2), 5.25 (dd, J = 10.65 Hz, 1.23 Hz, 1H,=CH), 5.33 (dd, J = 17.25 Hz, 1.49 Hz, 1H, = CH), 5.87−5.94 (, 1H, CH), 6.48 (br, 1H, NH), 7.00 (d, J = 7.02 Hz, 1H, NH); ^{13}C NMR (125 MHz, normal/DEPT-135): δ 18.11 (+ve, CH_3), 19.49 (+ve, CH_3), 19.56 (+ve, CH_3), 24.80 (−ve, CH_{2Pro}), 27.90 (−ve, CH_{2Pro}), 35.39 (+ve, CH), 42.02 (−ve, CH_{2Gly}), 46.47 (−ve, CH_{2Pro}), 48.36 (+ve, CH_{Ala}), 60.16 (+ve, CH_{Pro}), 65.95 (−ve, CH_2), 118.72 (−ve, = CH_2), 131.57 (+ve, = CH), 168.31 (C═O), 170.44 (C═O), 172.47 (C═O), 177.09 (C═O); HRMS (microTOF-QII, MS, ESI): calcd for $C_{17}H_{27}O_5N_3$ ([M + Na]$^+$) 376.1842, found 376.1850.

*4.2.17. Isobut-Gly-Pro-Ala-O-dimethylallyl (**16**).* Compound **16** was synthesized according to the general procedure F as a white solid, yield 73%, mp 149 °C; $[\alpha]_D^{25}$ −87.5° (0.4, $CHCl_3$); IR (ATR): 3257, 3078, 2974, 2124, 1729, 1632, 1558, 1453, 1237, 1043, 948, 685 cm^{-1}; ^{1}H NMR (500 MHz, $CDCl_3$, 25 °C, TMS): δ 1.17 (d, J = 6.88 Hz, 6H, 2 x CH_{Iso}), 1.40 (t, 3H, J = 7.15 Hz, CH_{3Ala}), 1.71 (s, 3H, CH_3), 1.76 (s, 1H, CH_3), 1.94−2.03 (m, 2H, CH_{2Pro}), 2.11−2.19 (m, 1H, CH_{2Pro}), 2.29−2.33 (m, 1H, CH_{2Pro}), 2.41−2.48 (m, 1H, CH), 3.42−3.47 (m, 1H, CH_{2Pro}), 3.56−3.60 (m, 1H, CH_{2Pro}), 3.96−4.00 (m, 1H, CH), 4.10−4.14 (m, 1H, CH), 447−4.53 (m, 2H, CH_2), 4.59−4.66 (m, 2H, CH_2), 5.31−5.34 (m, 1H, = CH), 6.51 (br, 1H, NH), 6.97 (d, J = 7.04 Hz, 1H, CH); ^{13}C NMR (125 MHz, normal/DEPT-135): δ 18.08 (+ve, CH_3), 18.22 (+ve, CH_3), 19.50 (+ve, CH_3), 19.56 (+ve, CH_3), 24.79 (−ve, CH_{2Pro}), 25.79 (+ve, CH_3), 28.02 (−ve, CH_{2Pro}), 35.38 (+ve, CH), 42.02 (−ve, CH_{2Gly}), 46.45 (−ve, CH_{2Pro}), 48.38 (+ve, CH_{Ala}), 60.19 (+ve, CH_{Pro}), 62.34 (−ve, CH_2), 118.01 (+ve, = CH), 139.81 (C), 168.23 (C═O), 170.41 (C═O), 172.84 (C═O), 177.10 (C═O); HRMS (microTOF-QII, MS, ESI): calcd for $C_{19}H_{31}O_5N_3$ ([M + Na]$^+$) 404.2155, found 404.2156.

*4.2.18. Isobut-Gly-Pro-Ala-O-Cinnamyl (**17**).* Compound **17** was synthesized according to the general procedure F as a white solid, yield 76%, mp 158 °C; $[\alpha]_D^{25}$ −95° (0.4, $CHCl_3$); IR (ATR): 3257, 3086, 2959, 2877, 2363, 2109, 1714, 1632, 1453, 1380, 1237, 1103, 984, 693, 521 cm^{-1}; ^{1}H NMR (500 MHz, $CDCl_3$, 25 °C, TMS): δ 1.17 (d, J = 6.85 Hz, 6H, 2 × CH_{Iso}), 1.44 (t, 3H, J = 7.18 Hz, CH_{3Ala}), 1.90−2.03 (m, 2H, CH_{2Pro}), 2.11−2.17 (m, 1H, CH_{2Pro}), 2.30−2.35 (m, 1H, CH_{2Pro}), 2.40−2.48 (m, 1H, CH_{Iso}), 3.43−3.45 (m, 1H, CH_{2Pro}), 3.56−3.60 (m, 1H, CH_{2Pro}), 3.96−3.97 (m, 1H, CH), 4.12−4.13 (m, 1H, CH), 4.55 (q, J = 7.28 Hz, 2H, OCH_2), 4.76−4.83 (m, 2H, CH_2), 6.24−6.29 (m, 1H, = CH), 6.48 (br, 1H, NH), 6.65−6.68 (m, 1H, = CH), 7.02−7.05 (m, 1H, NH), 7.27−7.28 (m, 1H, ArCH), 7.31−7.34 (m, 2H, ArCH), 7.38−7.40 (m, 2H, ArCH); ^{13}C NMR (125 MHz, normal/DEPT-135): δ 18.14 (+ve, CH_3), 19.45 (+ve, CH_3), 19.56 (+ve, CH_3), 24.79 (−ve, CH_{2Pro}), 27.92 (−ve, CH_{2Pro}), 35.38 (+ve, CH), 42.03 (−ve, CH_{2Gly}), 46.47 (−ve,CH_{2Pro}), 48.42 (+ve, CH_{Ala}), 60.17 (+ve, CH_{Pro}), 65.99 (−ve, CH_2), 122.46 (+ve, ArCH), 126.67 (+ve, ArCH), 128.65 (+ve, ArCH), 134.73 (+ve, CH), 136.02 (ArC), 168.31 (C═O), 170.47 (C═O), 172.60 (C═O), 177.12 (C═O); HRMS (microTOF-QII, MS, ESI): calcd for $C_{23}H_{31}O_5N_3$ ([M + Na]$^+$) 452.2155, found 452.2165.

*4.2.19. Isobut-Gly-Pro-Ala-O-Geranyl (**18**).* Compound **18** was synthesized according to the general procedure F as a white solid, yield 81%, mp 125 °C; $[\alpha]_D^{25}$ −50° (0.4, $CHCl_3$); IR (ATR): 3265, 3086, 2974, 2363, 2102, 1744, 1632, 1558, 1453, 1386, 1237, 1051, 946, 685, 603 cm^{-1}; ^{1}H NMR (500 MHz, $CDCl_3$, 25 °C, TMS): δ 1.16−1.18 (m, 6H, 2 × CH_{Iso}), 1.39−1.41 (m, 3H, CH_3), 1.58−1.62 (m, 3H, CH_3), 1.67−1.70 (m, 6H, 2 × CH_3), 1.91−2.09 (m, 6H, 2 × CH_{2Ger}), 2.15−2.19 (m, 1H, CH_{2Pro}), 2.24−2.30 (m, 1H, CH_{2Pro}), 2.41−2.50 (m, 1H, CH_{Iso}), 3.44 (q, J = 9.10 Hz, 1H, CH_{2Pro}), 2.43−2.49 (m, 1H, CH_{2Iso}), 3.45 (q, J = 9.56 Hz, 1H, CH_{2Pro}), 3.56−3.60 (m, 1H, CH_{2Pro}), 3.96−4.00 (m, 1H, CH), 4.10−4.15 (m, 1H, CH), 4.48−4.53 (m, 2H, CH_2), 4.63−4.66 (, 2H, CH_2), 5.07 (t, J = 6.54 Hz, 1H, CH), 5.32 (t, J = 6.50 Hz, 1H, CH), 6.53

https://doi.org/10.1021/acsomega.3c09069
ACS Omega 2024, 9, 12896−12913

(br, 1H, NH), 7.03 (br, 1H, NH); DEPT-135 NMR (125 MHz, normal): δ 16.51 (+ve, CH_3), 17.71 (+ve, CH_3), 18.21 (+ve, CH_3), 19.50 (+ve, CH_3), 19.56 (+ve, CH_3), 24.78 (−ve, CH_{2Pro}), 25.70 (+ve, CH_3), 26.23 (−ve, CH_{2Pro}), 28.06 (−ve, CH_2), 32.00 (−ve, CH_2), 35.36 (+ve, CH), 39.50 (−ve, CH_2), 42.01 (−ve,CH_2), 46.45 (−ve, CH_{2Pro}), 48.36 (+ve, CH_{Ala}), 60.17 (+ve, CH_{Pro}), 62.80 (−ve, CH_2), 117.71 (+ve, CH), 123.62 (+ve, CH), 165.75 (C=O), 168.45 (C=O), 170.57 (C=O), 172.14 (C=O), 177.19 (C=O); HRMS (microTOF-QII, MS, ESI): calcd for $C_{24}H_{39}O_5N_3$ ([M + H]$^+$) 472.2781, found 472.2779.

*4.2.20. Isobut-Gly-Pro-Ala-O-Crotyl (**19**).* Compound **19** was synthesized according to the general procedure F as a white solid, yield 80%, mp 136 °C; $[\alpha]_D^{25}$ −65° (0.4, $CHCl_3$); IR (ATR): 3257, 3086, 2981, 2124, 1722, 1632, 1558, 1453, 1244, 1148, 685, 484 cm^{-1}; ^{1}H NMR (500 MHz, $CDCl_3$, 25 °C, TMS): δ 1.17 (d, J = 6.93 Hz, 6H, 2 × CH_{Iso}), 1.30 (t, 3H, J = 7.40 Hz, CH_{3Cro}), 1.45 (d, J = 7.24 Hz, 3H, CH_{3Ala}), 1.92−1.98 (m, 1H, CH_{2Pro}), 2.00−2.05 (m, 1H, CH_{2Pro}), 2.09−2.17 (m, 1H, CH_{2Pro}), 2.32−2.36 (m, 1H, CH_{2Pro}), 2.43−2.49 (m, 1H, CH_{2Pro}), 3.45 (q, J = 9.56 Hz, 1H, CH), 3.57−3.61 (m, 1H, CH_{2Pro}), 3.97−4.02 (m, 1H, CH), 4.09−4.13 (m, 1H, CH), 4.19−4.23 (q, J = 7.12 Hz, 2H, OCH_2), 4.52−4.58 (m, 2H, CH_2), 4.76−4.84 (m, 2H, CH_2), 6.03−6.06 (m, 1H, CH), 6.50 (br, 1H, NH), 6.90−6.95 (m, 1H, CH), 7.13 (d, J = 7.36 Hz, 1H, NH); ^{13}C NMR (125 MHz, normal/DEPT-135): δ 14.23 (+ve, CH_{Cro}), 17.98 (+ve, CH_{3Ala}), 19.50 (+ve, CH_{3Iso}), 19.57 (+ve, CH_{3Cro}), 24.81 (−ve, CH_{2Pro}), 27.80 (−ve, CH_{2Pro}), 35.34 (+ve, CH), 42.02 (−ve, CH_{2Gly}), 46.52 (−ve, CH_{2Pro}), 48.33 (+ve, CH_{Ala}), 60.10 (+ve, CH_{Pro}), 60.72 (−ve, CH_2), 63.36 (−ve, OCH_2), 122.56 (+ve, CH), 140.40 (+ve, CH), 165.75 (C=O), 168.45 (C=O), 170.57 (C=O), 172.14 (C=O), 177.19 (C=O); HRMS (microTOF-QII, MS, ESI): calcd for $C_{20}H_{31}O_7N_3$ ([M + Na]$^+$) 448.2054, found 448.2087.

*4.2.21. Cbz-Gly-OH (**20**).* Compound **20** was synthesized according to the general procedure A as a white solid, yield 80%; mp 119 °C; HRMS (microTOF-QII, MS, ESI): calcd for $C_{10}H_{11}O_4N$ ([M + Na]$^+$) 232.0580, found 232.0539.

*4.2.22. Cbz-Gly-Pro-Ala-OMe (**21**).* Compound **21** was synthesized according to the general procedure C as a white solid, yield 75%, mp 129 °C; $[\alpha]_D^{25}$ −57.5° (0.4, $CHCl_3$); IR (ATR): 3309, 3085, 2944, 2363, 1714, 1550, 1453, 1237, 1155, 1058, 969, 879, 693, 462 cm^{-1}; ^{1}H NMR (500 MHz, $CDCl_3$, 25 °C, TMS): δ 1.38 (d, J = 7.15 Hz, 3H, CH_{3Ala}), 1.90−1.96 (m, 1H, CH_{2Pro}), 1.99−2.04 (m, 1H, CH_{2Pro}), 2.09−2.19 (m, 1H, CH_{2Pro}), 2.31−2.34 (m, 1H, CH_{2Pro}), 3.38−3.43 (m, 1H, CH_{2Pro}), 3.53−3.57 (m, 1H, CH_{2Pro}), 3.73 (s, 3H, OCH_3), 3.96−4.07 (m, 2H, CH_{2Gly}), 4.45−4.55 (m, 2H, CH_{Ala} + CH_{Pro}), 5.10−5.14 (m, 2H, CH_2), 5.71 (br, 1H, NH), 7.10 (d, J = 5.14 Hz, 1H, NH), 7.30−7.36 (m, 5H, ArH); ^{13}C NMR (125 MHz, normal/DEPT-135): δ 18.02 (+ve, CH_3), 24.86 (−ve, CH_{2Pro}), 27.66 (−ve, CH_{2Pro}), 43.46 (−ve, CH_{2Gly}), 46.38 (−ve,CH_{2Pro}), 48.27 (+ve, CH_{Ala}), 52.43 (+ve, CH_{Pro}), 60.12 (−ve, CH_2), 66.97 (−ve, CH_2), 128.05 (+ve, ArCH), 128.15 (+ve, ArCH), 128.52 (+ve, ArCH), 136.37 (ArC), 156.27 (C=O), 168.12 (C=O), 170.41 (C=O), 173.23 (C=O); HRMS (microTOF-QII, MS, ESI): calcd for $C_{19}H_{25}O_6N_3$ ([M + H]$^+$) 392.1816, found 392.1764.

*4.2.23. Cbz-Gly-Pro-Ala-OH (**22**).* Compound **22** was synthesized according to the general procedure D as a white solid, yield 79%, mp 119 °C; $[\alpha]_D^{25}$ −62.5° (0.4, $CHCl_3$); IR (ATR): 3280, 3063, 2885, 2646, 2363, 2109, 1699, 1647, 1535, 1446, 1237, 1058, 984, 924, 775 cm^{-1}; ^{1}H NMR (500 MHz, DMSO-d_6, 25 °C, TMS): δ 1.25 (d, J = 7.24 Hz, 3H, CH_{3Ala}), 1.74−1.77 (m, 1H, CH_{2Pro}), 1.81−1.90 (m, 3H, CH_{2Pro}), 1.95−2.00 (m, 1H, CH_{2Pro}), 3.49−3.52 (m, 1H, CH_{2Pro}), 3.73−3.88 (m, 2H, CH_{2Gly}), 4.12−4.15 (m, 1H, CH_{pro}), 4.32−4.34 (m, 1H, CH_{Ala}), 5.01−5.03 (m, 2H, CH_2), 7.29−7.33 (m, 3H, CH_{Ar}), 7.35−7.36 (m, 3H, CH_{Ar}), 8.18 (d, J = 7.35 Hz, 1H, NH), 8.44 (d, J = 7.37 Hz, 1H, NH); ^{13}C NMR (125 MHz, normal/DEPT-135): δ 17.51 (+ve, CH_{3Ala}), 24.64 (−ve, CH_{2Pro}), 29.44 (−ve, CH_{2Pro}), 43.11 (−ve, CH_{2Gly}), 46.17 (−ve, CH_{2Pro}), 47.85 (+ve, CH_{Ala}), 59.55 (+ve, CH_{Pro}), 65.81 (−ve, CH_2), 128.14 (+ve, ArCH), 128.81 (+ve, ArCH), 137.58 (ArC), 156.93 (C=O), 167.50 (C=O), 171.87 (C=O); HRMS (microTOF-QII, MS, ESI): calcd for $C_{19}H_{24}O_6N_2$ ([M + H]$^+$) 378.1659, found 378.1623.

*4.2.24. Cbz-Gly-Pro-Ala-O-Allyl (**23**).* Compound **23** was synthesized according to the general procedure F as a white solid, yield 79%, mp 92 °C; $[\alpha]_D^{25}$ −110° (0.4, $CHCl_3$); IR (ATR): 3309, 2858, 3063, 2952, 2363, 2109, 1744, 1647, 1535, 1446, 1326, 1252, 1155, 1058, 924, 834, 693, 603 cm^{-1}; ^{1}H NMR (500 MHz, $CDCl_3$, 25 °C, TMS): δ 1.40 (d, J = 7.18 Hz, 3H, CH_{3Ala}), 1.90−1.95 (m, 1H, CH_{2Pro}), 1.99−2.03 (m, 1H, CH_{2Pro}), 2.13−2.15 (m, 1H, CH_{2Pro}), 2.30−2.33 (m, 1H, CH_{2Pro}), 3.40−3.43 (m, 1H, CH_{2Pro}), 3.54−3.58 (m, 1H, CH_{2Pro}), 3.96−4.03 (m, 2H, CH_{2Gly}), 4.49−4.54 (m, 2H, CH_{Ala} + CH_{Pro}), 4.61−4.63 (m, 2H, OCH_2), 5.09−5.14 (m, 2H, CH_2), 5.24−5.34 (m, 2H, CH_{2Allyl}), 5.73 (br, IH, NH), 5.87−5.92 (m, 1H, CH_{Allyl}), 7.11 (br, 1H, NH), 7.31−7.33 (m, 5H, CH_{Ar}); ^{13}C NMR (125 MHz, normal/DEPT-135): δ 18.03 (+ve, CH_{3Ala}), 24.86 (−ve, CH_{2Pro}), 27.75 (−ve, CH_{2Pro}), 43.46 (−ve, CH_{2Gly}), 46.40 (−ve, CH_{2Pro}), 47.26 (+ve, CH_{Ala}), 60.12 (+ve, CH_{Pro}), 65.93 (−ve, CH_2), 66.98 (−ve, CH_{2Allyl}), 118.71 (−ve, CH_{2Allyl}), 128.06 (+ve, ArCH), 128.16 (+ve, ArCH), 128.54 (+ve, ArCH), 131.59 (+ve, ArCH), 136.34 (ab, ArC), 156.28 (C=O), 168.11 (C=O), 170.49 (C=O), 172.47 (C=O); HRMS (microTOF-QII, MS, ESI): calcd for $C_{21}H_{27}O_6N_3$ ([M + H]$^+$) 440.1792, found 440.1768.

*4.2.25. Cbz-Gly-Pro-Ala-O-dimethylallyl (**24**).* Compound **24** was synthesized according to the general procedure F as a brown thick oil, yield 83%; $[\alpha]_D^{25}$ −125° (0.4, $CHCl_3$); IR (ATR): 3354, 2929, 2832, 2363, 2102, 1662, 1513, 1297, 1237, 1036, 931, 827, 521 cm^{-1}; ^{1}H NMR (500 MHz, $CDCl_3$, 25 °C, TMS): δ 1.38 (t, 3H, J = 7.13 Hz, CH_{3Ala}), 1.70 (s, 3H, CH_3), 1.75 (s, 1H, CH_3), 1.91−1.94 (m, 1H, CH_{2Pro}), 1.97−2.01 (m, 1H, CH_{2Pro}), 2.11−2.15 (m, 1H, CH_{2Pro}), 2.30−2.32 (m, 1H, CH_{2Pro}), 3.38−3.43 (m, 1H, CH_{2Pro}), 3.54−3.57 (m, 1H, CH_{2Pro}), 3.95−4.07 (m, 2H, CH_2), 4.46−4.54 (m, 2H, CH_{Ala} + CH_{Pro}), 4.61−4.63 (m, 2H, OCH_2), 5.10−5.14 (m, 2H, CH_2), 5.31−5.33 (m, 1H, = CH), 5.73 (br, 1H, NH), 7.06 (m, J = 6.54 Hz, 1H, NH), 7.31−7.36 (m, 5H, ArH); ^{13}C NMR (125 MHz, normal/DEPT-135): δ 18.08 (+ve, CH_3), 18.15 (+ve, CH_3), 24.85 (−ve, CH_{2Pro}), 25.78 (+ve, CH_3), 27.79 (−ve, CH_{2Pro}), 43.46 (−ve, CH_{2Gly}), 46.37 (−ve, CH_{2Pro}), 48.40 (+ve, CH_{Ala}), 60.15 (+ve, CH_{Pro}), 62.30 (−ve, CH_2), 66.95 (−ve, CH_2), 118.05 (+ve, = CH), 128.04 (+ve, ArCH), 128.52 (+ve, ArCH), 136.37 (C) 139.75 (C), 156.26 (C=O), 168.02 (C=O), 170.37 (C=O), 172.79 (C=O), 177.10 (C=O); HRMS (microTOF-QII, MS, ESI): calcd for $C_{23}H_{31}O_6N_3$ ([M + Na]$^+$) 468.2105, found 468.2051.

*4.2.26. Cbz-Gly-Pro-Ala-O-cinnamyl (**25**).* Compound **25** was synthesized according to the general procedure F as a brown thick oil, yield 82%; $[\alpha]_D^{25}$ −87.5° (0.4, $CHCl_3$); IR

https://doi.org/10.1021/acsomega.3c09069
ACS Omega 2024, 9, 12896−12913

(ATR): 3295, 3056, 2959, 2885, 2363, 2109, 1997, 1744, 1640, 1535, 1453, 1244, 1148, 969, 834, 693, 603 cm^{-1}; ^1H NMR (500 MHz, $CDCl_3$, 25 °C, TMS): δ 1.41 (t, 3H, J = 7.20 Hz, CH_{3Ala}), 1.88−2.00 (m, 2H, CH_{2Pro}), 2.09−2.18 (m, 1H, CH_{2Pro}), 2.31−2.32 (m, 1H, CH_{2Pro}), 2.40−2.48 (m, 1H, CH_{Iso}), 3.37−3.42 (m, 1H, CH_{2Pro}), 3.53−3.56 (m, 1H, CH_{2Pro}), 3.95−4.06 (m, 2H, $CH_{Ala+Pro}$), 4.50−4.55 (m, 2H, CH_2), 4.74−4.81 (m, 2H, CH_2), 5.06−5.17 (m, 2H, CH_2), 5.73 (br, 1H, NH), 6.23−6.28 (m, 1H, = CH), 6.64−6.67 (m, 1H, = CH), 7.13 (d, J = 7.02 Hz, 1H, NH), 7.30−7.39 (m, 10H, ArCH); ^{13}C NMR (125 MHz, normal/DEPT-135): δ 18.06 (+ve, CH_3), 24.85 (−ve, CH_{2Pro}), 27.73 (−ve, CH_{2Pro}), 43.46 (−ve, CH_{2Gly}), 46.39 (−ve,CH_{2Pro}), 48.42 (+ve, CH_{Ala}), 60.12 (+ve, CH_{Pro}), 65.94 (−ve, CH_2), 66.96 (−ve, CH_2), 122.52 (+ve, ArCH), 126.67 (+ve, ArCH), 128.05 (+ve, ArCH), 128.15 (+ve, ArCH), 128.20 (+ve, ArCH), 128.53 (+ve, ArCH), 128.64 (+ve, ArCH), 134.68 (+ve, CH), 136.05 (ArC), 136.37 (ArC), 156.28 (C═O), 168.11 (C═O), 170.48 (C═O), 172.58 (C═O); HRMS (microTOF-QII, MS, ESI): calcd for $C_{27}H_{31}O_6N_3$ ([M + Na]$^+$) 516.2105, found 516.2094.

*4.2.27. Cbz-Gly-Pro-Ala-O-Geranyl (**26**).* Compound **26** was synthesized according to the general procedure F as a brown thick oil, yield 84%; $[\alpha]_D^{25}$ −72.5° (0.4, $CHCl_3$); IR (ATR): 3309, 3063, 2931, 2363, 2117, 1997, 1647, 1535, 1446, 1326, 1252, 1051, 745, 700, 574 cm^{-1}; ^1H NMR (500 MHz, $CDCl_3$, 25 °C, TMS): δ 1.38 (d, J = 7.20 Hz, 3H, CH_3), 1.59 (s, 3H, CH_3), 1.68 (d, J = 8.95 Hz, 6H, 2 x CH_{3Ger}), 1.91−2.15 (m, 7H, 3H of CH_{2Pro} + 2 × CH_{2Ger}), 2.30−2.32 (m, 1H, CH_{2Pro}), 3.38−3.43 (m, 1H, CH_{2Pro}), 3.53−3.57 (m, 1H, CH_{2Pro}), 3.95−4.08 (m, 2H, CH_{Ala} + CH_{Pro}), 4.46−4.53 (m, 2H, CH_2), 4.53−4.68 (m, 2H, CH_2), 5.05−5.08 (m, 1H, CH), 5.10−5.12 (m, 2H, CH_2), 5.30−5.33 (m, 1H, CH), 5.71 (br, 1H, NH), 7.03−7.04 (m, 1H, NH), 7.31−7.36 (m, 5H, ArCH); DEPT-135 NMR (125 MHz, normal): δ 16.51 (+ve, CH_3), 17.72 (+ve, CH_3), 18.16 (+ve, CH_3), 24.86 (−ve, CH_{2Pro}), 25.70 (+ve, CH_3), 26.25 (−ve, CH_2), 27.78 (−ve, CH_2), 39.50 (−ve, CH_2), 43.46 (−ve, CH_2), 46.37 (−ve, CH_2), 48.40 (+ve, CH), 60.15 (+ve, CH), 62.29 (−ve, CH_2), 66.95 (−ve, CH_2), 117.76 (+ve, CH), 123.66 (+ve, CH), 128.04 (+ve, ArCH), 128.41 (+ve, ArCH), 128.52 (+ve, ArCH), 131.90 (ArC), 136.37 (ArC), 142.97 (ArC), 156.25 (C═O), 168.01 (C═O), 170.35 (C═O), 172.79 (C═O); HRMS (microTOF-QII, MS, ESI): calcd for $C_{28}H_{39}O_6N_3$ ([M + H]$^+$) 536.2731, found 536.2697.

*4.2.28. Cbz-Gly-Pro-Ala-O-Crotyl (**27**).* Compound **27** was synthesized according to the general procedure F as a white solid, yield 81%, mp 103 °C; $[\alpha]_D^{25}$ −87.5° (0.4, $CHCl_3$); IR (ATR): 3302, 3063, 2987, 2363, 2117, 1997, 1722, 1446, 1654, 1535, 1259, 1155,, 1058, 976, 834, 611 cm^{-1}; ^1H NMR (500 MHz, $CDCl_3$, 25 °C, TMS): δ 1.29 (t, J = 7.09 Hz, 3H, CH_3), 1.43 (d, J = 7.22 Hz, 3H, CH_{3Cro}), 1.88−1.95 (m, 1H, CH_{2Pro}), 1.99−2.04 (m, 1H, CH_{2Pro}), 2.09−2.17 (m, 1H, CH_{2Pro}), 2.34−2.38 (m, 1H, CH_{2Pro}), 2.43−2.49 (m, 1H, CH_{2Pro}), 3.40 (q, J = 9.66 Hz, 1H, CH_{2Pro}), 3.54−3.58 (m, 1H, CH_{2Pro}), 3.97−4.07 (m, 2H, $CH_{Ala+Pro}$), 4.20 (q, J = 7.08 Hz, 2H, CH_2), 4.51−4.50 (m, 2H, CH_2), 4.78−4.80 (m, 2H, CH_2), 5.09−5.15 (m, 2H, CH_2), 5.72 (br, 1H, NH), 6.04 (d, J = 15.78 Hz, 1H, = CH), 6.92 (dt, J = 15.40 Hz, J = 4.60 Hz, 1H, = CH), 7.17 (d, J = 7.00 Hz, 1H, NH), 7.03−7.36 (m, 5H, ArH); ^{13}C NMR (125 MHz, normal/DEPT-135): δ 14.21 (+ve, CH_{Cro}), 17.94 (+ve, CH_{3Ala}), 24.88 (−ve, CH_{2Pro}), 27.49 (−ve, CH_{2Pro}), 43.46 (−ve, CH_{2Gly}), 46.43 (−ve, CH_{2Pro}), 48.35 (+ve, CH_{Ala}), 60.08 (+ve, CH_{Pro}), 60.69 (−ve, CH_2), 63.34 (−ve, OCH_2), 67.00 (−ve, CH_2), 122.58 (+ve, CH), 128.06 (+ve, ArCH), 128.17 (+ve, ArCH), 128.53 (+ve, ArCH), 136.34 (ArC), 140.40 (+ve, CH), 165.75 (C═O), 168.45 (C═O), 168.30 (C═O), 170.46 (C═O), 172.08 (C═O); HRMS (microTOF-QII, MS, ESI): calcd for $C_{24}H_{31}O_8N_3$ ([M + H]$^+$) 512.2003, found 512.2002.

*4.2.29. Boc-Gly-OH (**28**).* Compound **28** was synthesized according to the general procedure A as a colorless liquid; yield 90%.

*4.2.30. Boc-Gly-Pro-Ala-OMe (**29**).* Compound **29** was synthesized according to the general procedure C as a white solid; yield 40%, mp 155 °C; ^1H NMR (500 MHz, $CDCl_3$, 25 °C, TMS): δ 1.40 (d, J = 6.72 Hz, 3H, CH_{3Ala}), 1.45 (s, 9H, CH_{3Boc}), 1.88−1.95 (m, 1H, CH_{2Pro}), 2.12−2.14 (m, 1H, CH_{2Pro}), 2.33−2.37 (m, 1H, CH_{2Pro}), 3.39−3.41 (m, 1H, CH_{2Pro}), 3.52−3.56 (m, 1H, CH_{2Pro}), 3.74 (s, 3H, OCH_3), 3.89−4.01 (m, 2H, CH_2), 4.47−4.50 (m, 1H, CH_{2Pro}), 4.55−4.57 (m, 1H, CH), 5.42−5.44 (m, 1H, CH), 6.74 (d, J = 7.24 Hz, 1H, NH), 7.15 (d, J = 6.71 Hz, 1H, NH); ^{13}C NMR (125 MHz, normal/DEPT-135): δ 18.04 (+ve, CH_{3Ala}), 24.89 (−ve, CH_{2Pro}), 27.53 (−ve, CH_{2Pro}), 28.34 (+ve, CH_{3Boc}), 43.11 (−ve, CH_{2Gly}), 46.35 (−ve, CH_{2Pro}), 48.27 (+ve, CH_{Ala}), 52.46 (+ve, OCH_3), 60.06 (+ve, CH_{Pro}), 79.82 (+ve, C), 155.83 (C═O), 168.64 (C═O), 170.46 (C═O), 173.27 (C═O); HRMS (microTOF-QII, MS, ESI): calcd for $C_{16}H_{27}O_6N_3$ ([M + Na]$^+$) 380.1792, found 380.1792.

*4.2.31. NH_2-Gly-Pro-Ala-OMe (**30**).* Compound **30** was synthesized according to the general procedure E as a light-yellow-colored liquid, yield 90%; $[\alpha]_D^{25}$ −132.5° (0.4, MeOH); IR (ATR): 3265, 3071, 2959, 2363, 2102, 1654, 1535, 1461, 1358, 1192, 984, 924, 834, 775, 514 cm^{-1}; ^1H NMR (500 MHz, $CDCl_3$, 25 °C, TMS): δ 1.29 (d, J = 7.27 Hz, 3H, CH_{3Ala}), 1.90−1.91 (m, 3H, CH_{2Pro}), 2.04−2.10 (m, 1H, CH_{2Pro}), 3.53−3.54 (m, 2H, CH_{2Pro}), 3.62 (s, 3H, OCH_3), 3.78−3.83 (m, 2H, CH_2), 4.20−4.26 (m, 1H, CH_{Pro}), 4.39 (dd, J = 8.71 Hz, 2.60 Hz, 1H, CH), 8.31 (br, NH_2), 8.47 (d, J = 7.33 Hz, 1H, NH); ^{13}C NMR (125 MHz, normal/DEPT-135): δ 17.29 (+ve, CH_{3Ala}), 24.44 (−ve, CH_{2Pro}), 29.73 (−ve, CH_{2Pro}), 40.30 (−ve, CH_{2Gly}), 46.27 (−ve, CH_{2Pro}), 47.96 (+ve, CH_{Ala}), 52.36 (+ve, OCH_3), 59.55 (+ve, CH_{Pro}), 164.83 (C═O), 171.58 (C═O), 173.40 (C═O); HRMS (microTOF-QII, MS, ESI): calcd for $C_{11}H_{19}O_4N_3$ ([M + H]$^+$) 258.1448, found 258.1457.

*4.2.32. 2,2′-Bis(prop-2-yn-1-yloxy)-1,1′-binaphthalene (**31**).* Compound **31** was synthesized according to the general procedure G as a thick liquid; yield 95%; HRMS (microTOF-QII, MS, ESI): calcd for $C_{26}H_{18}O_2$ [M + Na]$^+$ 385.4097, found 385.4070.

*4.2.33. (3-Azidoallyl)benzene (**32**).* Compound **32** was synthesized according to the general procedure H as a yellowish-brown thick liquid; yield 80%; IR (KBr): 3459, 2862, 3028, 2937, 2094, 1886, 1736, 1669, 1490, 1386, 1237, 1088, 989, 879, 745, 693, 559 cm^{-1}.

*4.2.34. 2,2′-Bis((1-((E)-3-phenylprop-1-en-1-yl)-1H-1,2,3-triazol-5-yl)methoxy)-1,1′-binaphthalene (**33**).* Compound **33** was synthesized according to the general procedure I as a yellowish-brown thick liquid, yield 95%; IR (KBr): 2922, 1595.2, 1326, 1215, 1043, 805, 752 cm^{-1}. ^1H NMR (500 MHz, $CDCl_3$) δ: 1.23−1.25 (s, 1H, CH), 2.02−2.06 (d, J = 16 Hz, 1H, CH), 4.80−4.81 (s, 4H, CH_2), 5.04−5.07 (m, 2H, CH_2), 5.17−5.19 (m, 2H, CH_2), 6.04−6.10 (m, 2H, ArH), 6.45 (s, 1H, ArH), 6.49 (s, 2H, ArH), 7.12 (s, 4H, ArH), 7.19−7.22

https://doi.org/10.1021/acsomega.3c09069
ACS Omega 2024, 9, 12896−12913

(m, 1H, ArH), 7.28−7.36 (m, 8H, ArH), 7.42−7.44 (d, J = 10 Hz, 2H, ArH), 7.68−7.69 (d, J = 5 Hz, 2H, ArH), 7.73−7.75 (d, J = 10 Hz, 2H, ArH); ^{13}C NMR (125 MHz, normal/DEPT-135) δ: 14.32 (+ve, CH), 20.81 (+ve, CH), 21.07 (+ve, CH), 48.01 (−ve, CH_2), 52.15 (−ve, CH_2), 64.00 (−ve, CH_2), 64.08 (−ve, CH_2), 115.8 (+ve, ArCH), 115.99 (+ve, ArCH), 120.67 (+ve, ArC), 121.53 (+ve, ArCH), 122.19 (+ve, ArCH), 123.92 (+ve, ArCH), 125.35 (+ve, ArCH), 126.45 (+ve, ArCH), 126.80 (+ve, ArCH), 127.97 (+ve, ArCH), 128.63 (+ve, ArCH), 128.67 (+ve, ArC), 128.68 (+ve, ArCH), 128.80 (+ve, ArC), 128.81 (+ve, ArCH), 129.50 (+ve, ArCH), 129.51 (+ve, ArC), 133.90 (+ve, ArC), 134.06 (+ve, ArC), 135.34 (+ve, ArC). HRMS (microTOF-QII, MS, ESI): calcd for $C_{44}H_{36}O_2N_6$ ([M + H]$^+$) 681.2772, found 681.2766.

4.3. AChE Inhibition Assay. The in vitro AChE activity of synthesized compounds was evaluated using the Ellman assay.[31] Donepezil was used as a reference compound. Human AChE, acetylthiocholine iodide (ATChI), and 5,5′-dithio-bis(2-nitrobenzoic acid) (DTNB) were obtained from Sigma-Aldrich. Stock solutions of 10^{-3} M concentration of all of the compounds were made in DMSO, and further dilutions to obtain the concentration range of 10^{-5}−10^{-8} M were made in PBS buffer. AChE was dissolved in PBS (NaH_2PO_4/Na_2HPO_4) buffer to obtain a solution of 2.5 units/mL at pH 7.2. DTNB and ATChI solutions of 0.3 mM and 10 mM concentrations, respectively, were prepared in PBS buffer. 20 μL of AChE and 140 μL of DTNB (0.3 mM) solutions were added to the 96-well plate with or without test compounds (20 μL). The blank well contains all of the components as in the test wells except for the enzyme. The resulting reaction mixture was incubated at 25 °C for 20 min, followed by the addition of 20 μL of ATChI solution (10 mM). The absorbance of the reaction mixture at 412 nm was recorded on a microplate reader (Synergy BioTek 96-well microplate reader) at 1 min interval for a total of 10 min. All experiments were run in triplicate. The %age inhibition of the enzyme by the respective test compounds was determined using the equation $100 - (T/C) \times 100$, where T and C represent enzyme activity with or without the test compound, respectively. IC_{50} values were obtained graphically and are reported as mean ± SEM.

4.4. BACE-1 inhibition assay. The BACE-1 fluorescence resonance energy transfer (FRET) assay kit was purchased from Sigma-Aldrich, and the assay was performed according to the supplier's protocol. Stock solutions of the substrate (500 μM) and the test compounds (10 mM) were prepared using DMSO and kept at 20 °C. Further dilutions of the test compounds were done in a fluorescent assay buffer (FAB) supplied in the kit. BACE-1 enzyme solution (0.3 unit/L) and 50 μM substrate solution were produced by diluting with the fluorescent assay buffer just before starting the experiment. With excitation at 320 nm and emission at 405 nm, the fluorometer was set to the well plate reader mode. In the assay, a 96-well black polystyrene microplate was filled with 10 μL of the test compound, 20 μL of substrate, and 68 μL of FAB. The time zero reading of fluorescence was measured immediately after the addition of 2 μL of BACE-1. Then, the plate was incubated at 37 °C and the fluorescence was measured after 2 h. Triplicates of each concentration were tested. In the control wells, all chemical reagents except for BACE-1 were added. The background signal was measured using the fluorescence readings of the control wells and subtracted from all of the wells containing test compounds. Also, the fluorescence readings of the assay solutions without inhibitors were taken. The following expression was used to compute the percentage of inhibition caused by the presence of the test compound: 100- (Fi/Fo x 100), where Fi and Fo are the fluorescence intensities obtained in the presence and absence of inhibitors, respectively.

Calbiochem IV (CAS no. 797035-11-1) was taken as the reference drug with IC_{50} of 18 nM (literature value).

4.5. Inhibition of Aβ_{1-42} Aggregation. Inhibition of Aβ_{1-42} aggregation by the synthesized compounds was evaluated using a Thioflavin-T (ThT) fluorometric assay.[41] Recombinant human HFIP-pretreated Aβ_{1-42} peptide (7.5 μM) was prepared in 150 mM HEPES buffer of pH 7.4. Donepezil was used as the standard drug. Stock solutions of concentration 100 μM of all of the test compounds along with donepezil were prepared in HEPES buffer. 20 μL of HFIP (7.5 μM) was mixed with 10 μL of the test compounds and donepezil and subsequently added to the corresponding wells of black-walled 96-well plates in quadruplicate. Then, 70 μL of ThT solution of 14.3 μM concentration was added to each well, making a final volume of 100 μL in each well. The kinetic experiment with an excitation wavelength of 440 nm and emission wavelength of 490 nm for 48 h was run on a 96-well microplate reader (Synergy Hybrid reader, BioTek Instruments). The ThT fluorescence through the bottom of the plate was measured every 3 min with a medium continuously shaking between the measurements. The fluorescence intensities at the plateau were averaged for all of the test compounds, and the average fluorescence at t = 0 h was subtracted. The percentage inhibition of the Aβ_{1-42} self-induced aggregation was calculated using the formula

$$\%\text{inhibition} = \left(1 - \frac{F_i}{F_0}\right)100$$

where F_i is the increase in fluorescence of Aβ_{1-42} treated with the test compounds and F_0 is the increase in the fluorescence of Aβ_{1-42} alone.

4.6. PAMPA. The used 96-well precoated PAMPA Plate System Gentest was obtained from Corning (Catalog number 353015). Caffeine and norfloxacin were used as the reference compounds. Solutions of all of the tested compounds (200 μM) were prepared in PBS buffer (pH 7.4). 300 μL of the test compound solution was added to the donor wells, whereas 200 μL of buffer was added to all wells of the acceptor plate. All of the compounds were tested in triplicate. The plate was incubated for 5 h at room temperature. Then, 150 μL was aspirated from each well, and the concentrations of the compounds in the acceptor and donor wells were calculated with LC-MS. The permeability coefficients (Pe) were calculated according to the formulas given in the protocol. According to the PAMPA plate's manufacturer, compounds with Pe values higher than 1.5×10^{-6} cm/s possess good human oral absorption capacity.

4.7. Molecular Docking. Molecular docking studies were performed by using the Schrödinger software package (Schrödinger Release 2015-4: Maestro, version 10.0, Schrödinger, LLC). The 3D crystal coordinates of AChE, BACE-1, and Aβ were retrieved from the protein data bank (www.rcsb.org) with pdb IDs 1EVE, 4B05, and 1IYT, respectively. The proteins were preprocessed, polar hydrogens were added, and water molecules were removed. Taking into account the drug solubility and permeability, the heteroatoms were ionized at biological pH. To reduce steric clashes by amino acids,

https://doi.org/10.1021/acsomega.3c09069
ACS Omega 2024, 9, 12896−12913

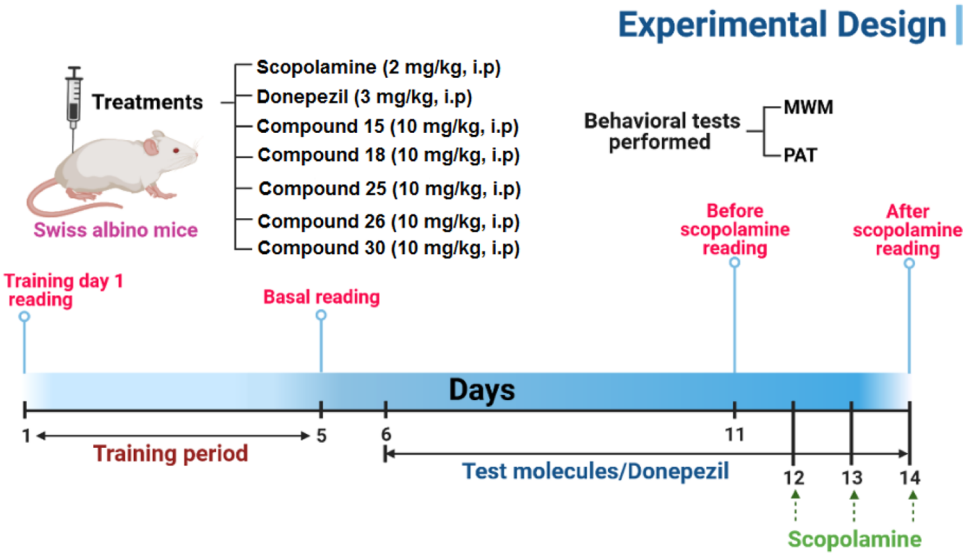

Figure 8. Overall experimental design for the memory test of the animals.

hydrogen bonds were optimized. Using the Ligprep tool of Schrödinger, ligands were prepared, which adapt a 3D structure. Prior to docking, a cubic grid dimension with various dimensions with the grid points along the *x*, *y*, and *z* axes was generated with a van der Waals radius of 1. The ligands were then docked into the generated grids, and the interactions of the prepared ligand with the receptor were calculated using the XP ligand docking in glide. Interactions between ligands and enzymes were analyzed, and hydrogen atoms that are nonpolar were merged to carbon atoms. The docking procedure was validated by docking the cocrystallized ligands of AChE and BACE-1 in the respective enzymes, and RMSD was calculated.

4.8. Animal Studies. Swiss albino mice (25−30 g) were purchased from the Indian Institute of Integrative Medicine, Jammu, India. During the entire studies, animals had free access to water and feed. All of the animal experiments were approved by the Institutional Animal Ethics Committee constituted under CPCSEA with reference no. 226/CPCSEA/2019/47.

4.9. Experiment Design for Behavioral Analysis. The Morris water maze (MWM) test and the passive avoidance task (PAT) were used for the behavioral studies of mice in order to evaluate the effect of the new compounds. In this study, mice were placed into eight groups, each having five animals. Group 1 was taken as the control, and groups 2−8 were given scopolamine, donepezil, compound **15**, compound **18**, compound **25**, compound **26**, and compound **30**, respectively. The animals were trained for 4 days in the MWM test. On the fifth day, the basal readings were taken. The untrained animals were excluded from the studies. Various interventions (0.2 mL of 10 mg/kg conc) were given for a total of 9 days, starting from day 6. Scopolamine (2 mg/kg, i.p.) treatment was given half an hour prior to the various interventions on the 12th, 13th, and 14th days of the experiment. The behavioral observation was taken on day 11 (before scopolamine treatment) and day 14 (after scopolamine treatment). On the 14th day, 1 h after behavioral analysis, the animals were sacrificed and the brain tissues were harvested for biochemical tests.[42] The overall experimental design is illustrated in Figure 8.

4.10. Morris Water Maze (MWM) Test. Morris water maze is a circular tank having 90 cm diameter and 50 cm height. The tank is divided into four quadrants with Any-Maze software. One out of the four quadrants has a circular platform of 9 cm diameter. The tank was filled with water (maintained at 25 °C) in such a manner that the water level remains 2 cm above the platform. To hide the platform, the water in the tank was made opaque with nontoxic colors. The camera connected to Any-Maze software was mounted above the tank. The track of animal movement was recorded with software (ANY-maze 5.7, Ugo Basile, Italy). A 10 s of stay on the platform was regarded as a correct entry. A latency to reach the platform was taken as a measure of animal memory.[43]

4.11. Passive Avoidance Task (PAT). The passive avoidance task apparatus is a square box equipped with small electrical rods on the floor having a square-shaped shock-free area. The electrical rods were kept on a low-intensity current, and the animal was placed in one corner of the apparatus. The animal was placed on the grid floor, and a low-intensity current was supplied to the grid. The latency to reach a shock-free area (s) was recorded and taken as a measure of animal memory. A correct entry to the shock-free area was registered if all of the paws of mice were on the shock-free area.[44]

4.12. Plasma Stability Assay. A stock solution of compound **25** (5 mM) was prepared in DMSO. Ultrapure water was used to prepare PBS buffer (pH 7.4; 0.01M, 0.8 g of NaCl, 0.03 g of KCl, 0.14 g of Na_2HPO_4, 0.024 KH_2PO_4). A solution of compound **25** in PBS (50 μM) was used as the positive control. Plasma was extracted by centrifuging the blood sample at 3000 rpm for 15 min at 4 °C. Then, the supernatant was collected using a micropipette and stored at −20 °C. Before its use, plasma was centrifuged at 2000 rpm for 10 min to remove fibrous precipitates resulting from freezing, and the supernatant was retained. Plasma (pH 7−8) was treated with **25** to produce the solution of final concentration 50 μM. After incubation of the sample at 37 °C for 1 and 12 h, 400 μL of acetonitrile was added to quench the reaction. Then, the sample was centrifuged at 10,000 rpm at room temperature for 15 min and the supernatant was separated. To quantify the concentration of the compound in plasma, 100 μL of treated supernatant and buffer solutions were injected into the

https://doi.org/10.1021/acsomega.3c09069
ACS Omega 2024, 9, 12896−12913

spectrometer using an autosampler. The mobile phase gradient comprised 100% acetonitrile. The spectra were recorded in the positive ion mode. The percentage of analyte lysed by the plasma of each solution was calculated from intensities of peaks observed from the HRMS spectra at the same interval of time using eq 1, where I_0 and I represent the intensities of the compound in the presence of buffer and plasma (treated supernatant). Remarkably, a slight change in the concentration of **25** (∼10%) was observed after a long time of incubation (12 h). It is demonstrated that plasma had no remarkable effect on the half-life time of **25**, and further, it can be prioritized for in vivo studies.

4.13. Lipinski Parameters. Lipinski parameters and ADME properties of the designed compounds were checked using online softwares Molinspiration[45] and PreADMET,[46] respectively.

■ ASSOCIATED CONTENT

Supporting Information

The Supporting Information is available free of charge at https://pubs.acs.org/doi/10.1021/acsomega.3c09069.

^{1}H and ^{13}C NMR spectra, mass spectra, IR spectra and molecular docking data (PDF)

Three-dimensional model of target−ligand (compounds docked in BACE-1) (ZIP)

Three-dimensional model of target−ligand (compounds docked in AChE) (ZIP)

PDB coordinates for computational models (ZIP)

Molecular formula strings (CSV)

■ AUTHOR INFORMATION

Corresponding Author

Palwinder Singh − *Department of Chemistry, Guru Nanak Dev University, Amritsar 143005, India;* orcid.org/0000-0003-2332-5257; Email: palwinder_singh_2000@yahoo.com

Authors

Baljit Kaur − *Department of Chemistry, Guru Nanak Dev University, Amritsar 143005, India;* Present Address: Medicinal Chemistry, Virginia Commonwealth University, 300 West Franklin Street, Richmond, Virginia 23220, United States; orcid.org/0000-0002-0461-6692

Rajbir Kaur − *Department of Chemistry, Guru Nanak Dev University, Amritsar 143005, India*

Vivesh − *Department of Chemistry, Guru Nanak Dev University, Amritsar 143005, India*

Sudesh Rani − *Department of Chemistry, Guru Nanak Dev University, Amritsar 143005, India*

Rajbir Bhatti − *Department of Pharmaceutical Sciences, Guru Nanak Dev University, Amritsar 143005, India;* orcid.org/0000-0002-5761-7074

Complete contact information is available at: https://pubs.acs.org/10.1021/acsomega.3c09069

Notes

The authors declare no competing financial interest.

■ ACKNOWLEDGMENTS

Financial assistance from SERB-DST, New Delhi, is gratefully acknowledged. B.K. and R.K. thank CSIR, New Delhi, and Vivesh thanks SERB-DST, New Delhi, for fellowships. UGC, New Delhi, is gratefully acknowledged for financial grant to GNDU under University with Potential for Excellence Programme.

■ ABBREVIATIONS

CNS, central nervous system; AD, Alzheimer's disease; BACE-1, β-site APP cleaving enzyme 1; AChE, acetylcholine esterase; PNS, peripheral nervous system; Boc, *t*-butyloxycarbonyl; TEA, triethylamine; ECF, ethyl chloroformate; ACN, acetonitrile; Cbz, benzyloxy carbonyl; THF, tetrahydrofuran; DCM, dichloromethane; DMF, dimethylformamide; Aβ, amyloid β; PAMPA, β-site APP cleaving enzyme 1; MWM, Morris water maze; PAT, passive avoidance task; ADME, absorption distribution metabolism excretion; IC_{50}, concentration for 50% inhibition; TPSA, total polar surface area; log *P*, partition coefficient; TLC, thin-layer chromatography; SEM, standard error mean; i.p., intraperitoneally; DMSO, dimethyl sulfoxide; TFA, trifluoroacetic acid

■ REFERENCES

(1) Salgado, A. *Handbook of Innovations in Central Nervous System Regenerative Medicine*; Elsevier Science, 2020.

(2) Marshall, M. Roots of mental illness. *Nature* **2020**, *581*, 19−21.

(3) Taylor, P.; Brown, J. H. Acetylcholine. In *Basic Neurochemistry: Molecular, Cellular and Medical Aspects*, 6th ed.; Albers, R. W.; Siegel, G. J.; Katzman, R.; Agranoff, B. W., Eds.; Lippincott-Raven Publishers: Philadelphia, 1999.

(4) World Health Organization. Dementia. https://www.who.int/news-room/fact-sheets/detail/dementia (accessed August, 2021).

(5) Livingston, G.; Huntley, J.; Sommerlad, A.; Ames, D.; Ballard, C.; Banerjee, S.; Brayne, C.; Burns, A.; Cohen-Mansfield, J.; Cooper, C.; Costafreda, S. G.; Dias, A.; Fox, N.; Gitlin, L. N.; Howard, R.; Kales, H. C.; Kivimäki, M.; Larson, E. B.; Ogunniyi, A.; Orgeta, V.; Ritchie, K.; Rockwood, K.; Sampson, E. L.; Samus, Q.; Schneider, L. S.; Selbæk, G.; Teri, L.; Mukadam, N. Dementia prevention, intervention, and care: 2020 report of the lancet commission. *Lancet* **2020**, *396*, 413−446.

(6) Francis, P. T. The interplay of neurotransmitters in alzheimer's disease. *CNS Spectrum* **2005**, *10*, 6−9.

(7) Rodrigues, R.; Petersen, R. B.; Perry, G. Parallels between major depressive disorder and alzheimer' s disease: role of oxidative stress and genetic vulnerability. *Cell. Mol. Neurobiol.* **2014**, *34*, 925−949.

(8) Biringer, R. G. The role of eicosanoids in alzheimer' s disease. *Int. J. Environ. Res. Public Health* **2019**, *16*, 2560.

(9) Felger, J. C.; Lotrich, F. E. Inflammatory cytokines in depression: Neurobiological mechanisms and therapeutic implications. *Neuroscience* **2013**, *246*, 199−229.

(10) Maia, M. A.; Sousa, E. BACE-1 and γ-secretase as therapeutic targets for alzheimer's disease. *Pharmaceuticals* **2019**, *12*, 41.

(11) Jeppsson, F.; Eketjäll, S.; Janson, J.; Karlström, S.; Gustavsson, S.; Olsson, L. L.; Radesäter, A. C.; Ploeger, B.; Cebers, G.; Kolmodin, K.; Swahn, B. M.; Von Berg, S.; Bueters, T.; Fälting, J. Discovery of AZD3839, a potent and selective bace1 inhibitor clinical candidate for the treatment of alzheimer disease. *J. Biol. Chem.* **2012**, *287*, 41245−41257.

(12) Eketjäll, S.; Janson, J.; Kaspersson, K.; Bogstedt, A.; Jeppsson, F.; Fälting, J.; Haeberlein, S. B.; Kugler, A. R.; Alexander, R. C.; Cebers, G. AZD3293: A novel, orally active BACE1 inhibitor with high potency and permeability and markedly slow off-rate kinetics. *J. Alzheimer's Dis.* **2016**, *50*, 1109−1123.

(13) Yan, R. Stepping closer to treating alzheimer's disease patients with BACE1 inhibitor drugs. *Transl. Neurodegener.* **2016**, *5*, 13.

(14) Lopez, C. L.; Tariot, P. N.; Caputo, A.; Langbaum, J. B.; Liu, F.; Riviere, M. E.; Langlois, C.; Rouzade-Dominguez, M. L.; Zalesak, M.; Hendrix, S.; Thomas, R. G.; Viglietta, V.; Lenz, R.; Ryan, J. M.; Graf, A.; Reiman, E. M. The alzheimer's prevention initiative generation program: Study design of two randomized controlled trials for

individuals at risk for clinical onset of alzheimer's disease. *Alzheimer's Dement. Transl. Res. Clin. Interventions* **2019**, *5*, 216−227.
(15) Oehlrich, D.; Prokopcova, H.; Gijsen, H. J. M. The evolution of amidine-based brain penetrant bace1 inhibitors. *Bioorg. Med. Chem. Lett.* **2014**, *24*, 2033−2045.
(16) Liu, M.-Y.; Meng, S.; Wu, H.; Wang, S.; Wei, M.-J. Pharmacokinetics of single-dose and multiple-dose memantine in healthy chinese volunteers using an analytic method of liquid chromatography-tandem mass spectrometry. *Clin. Ther.* **2008**, *30*, 641−653.
(17) Brodaty, H.; Corey-Bloom, J.; Potocnik, F. C. V.; Truyen, L.; Gold, M.; Damaraju, C. R. V. Galantamine prolonged-release formulation in the treatment of mild to moderate alzheimer's disease. *Dement. Geriatr. Cogn. Disord.* **2005**, *20*, 120−132.
(18) Jarrott, B. Tacrine: in vivo veritas. *Pharmacol. Res.* **2017**, *116*, 29−31.
(19) Rehfeldt, S. C. H.; Majolo, F.; Goettert, M. I.; Laufer, S. c-Jun N-Terminal kinase inhibitors as potential leads for new therapeutics for alzheimer's diseases. *Int. J. Mol. Sci.* **2020**, *21*, No. 9677.
(20) Medda, F.; Smith, B.; Gokhale, V.; Shaw, A. Y.; Dunckley, T.; Hulme, C. Beyond Secretases: Kinase Inhibitors for the Treatment of Alzheimer's Disease. *Annu. Rep. Med. Chem.* **2013**, *48*, 57−71.
(21) De Simone, A.; Tumiatti, V.; Andrisano, V.; Milelli, A. Glycogen synthase kinase 3β: a new gold rush in anti-alzheimer's disease multitarget drug discovery? *J. Med. Chem.* **2021**, *64*, 26−41.
(22) Korabecny, J.; Spilovska, K.; Soukup, O.; Spilovska, K.; Soukup, O.; Dolezal, R.; Kuca, K. Amyloid Beta Hypothesis: Attention to β- and γ-Secretase Modulators. In *Alzheimer's Disease − The 21st Century Challenge*; Dorszewska, J.; Kozubski, W., Eds.; IntechOpen, 2018; pp 1−20.
(23) Murphy, M. P.; Levine, H. Alzheimer's disease and the amyloid-β peptide. *J. Alzheimer's Dis.* **2010**, *19*, 311−323.
(24) Ahmed, R. R.; Holler, C. J.; Webb, R. L.; Li, F.; Beckett, T. L.; Murphy, M. P. BACE1 and BACE2 enzymatic activities in alzheimer's disease. *J. Neurochem.* **2010**, *112*, 1045−1053.
(25) Albert, J. S. *Progress in Medicinal Chemistry*; Lawton, G.; Witty, D. R., Eds.; Elsevier, 2009; Vol. *48*, Chapter 4, pp 133−161.
(26) Lane, R. M.; Potkin, S. G.; Enz, A. Targeting acetylcholinesterase and butyrylcholinesterase in dementia. *Int. J. Neuropsychopharmacol.* **2006**, *9*, 101−124.
(27) Tripathi, A.; Srivastava, U. Acetylcholinesterase: a versatile enzyme of nervous system. *Ann. Neurosci.* **2008**, *15*, 106−111.
(28) Bourne, Y.; Taylor, P.; Radić, Z.; Marchot, P. Structural insights into ligand interactions at the acetylcholinesterase peripheral anionic site. *EMBO J.* **2003**, *22*, 1−12.
(29) Deng, Y.; Jiang, Y.; Zhao, X.; Wang, J. Design, synthesize and bio-evaluate 1,2-dihydroisoquinolin- 3(*4H*)-one derivates as acetylcholinesterase and β-secretase dual inhibitors in treatment with alzheimer's disease. *J. Biosci. Med.* **2016**, *04*, 112−123.
(30) Green, K. D.; Fosso, M. Y.; Garneau-Tsodikova, S. Multifunctional donepezil analogues as cholinesterase and BACE1 inhibitors. *Molecules* **2018**, *23*, No. 3252.
(31) Nuthakki, V. K.; Sharma, A.; Kumar, A.; Bharate, S. B. Identification of embelin, a 3-undecyl-1,4-benzoquinone from *Embelia ribes* as a multitargeted anti-alzheimer agent. *Drug Dev. Res.* **2019**, *80*, 655−665.
(32) Han, J.; Ji, Y.; Youn, K.; Lim, G.; Lee, J.; Kim, D. H.; Jun, M. Baicalein as a potential inhibitor against BACE1 andAChE: Mechanistic comprehension through in vitro and computational approaches. *Nutrients* **2019**, *11*, 2694.
(33) Cen, J.; Guo, H.; Hong, C.; Lv, J.; Yang, Y.; Wang, T.; Fang, D.; Luo, W.; Wang, C. Development of tacrine-bifendate conjugates with improved cholinesterase inhibitory and pro-cognitive efficacy and reduced hepatotoxicity. *Eur. J. Med. Chem.* **2018**, *144*, 128−136.
(34) Pachón-Angona, I.; Refouvelet, B.; Andrýs, R.; Martin, H.; Luzet, V.; Iriepa, I.; Moraleda, I.; Diez-Iriepa, D.; Oset-Gasque, M. J.; Marco-Contelles, J.; Musilek, K.; Ismaili, L. Donepezil + chromone + melatonin hybrids as promising agents for alzheimer's disease therapy. *J. Enzyme Inhib. Med. Chem.* **2019**, *34*, 479−489.
(35) Neumann, U.; Ufer, M.; Jacobson, L. H.; Rouzade-Dominguez, M.; Huledal, G.; Kolly, C.; Lüönd, R. M.; Machauer, R.; Veenstra, S. J.; Hurth, K.; Rueeger, H.; Tintelnot-Blomley, M.; Staufenbiel, M.; Shimshek, D. R.; Perrot, L.; Frieauff, W.; Dubost, V.; Schiller, H.; Vogg, B.; Beltz, K.; Avrameas, A.; Kretz, S.; Pezous, N.; Rondeau, J.; Beckmann, N.; Hartmann, A.; Vormfelde, S.; David, O. J.; Galli, B.; Ramos, R.; Graf, A.; Lopez, C. L. The BACE-1 inhibitor CNP 520 for prevention trials in alzheimer's disease. *EMBO Mol. Med.* **2018**, *10*, No. e9316.
(36) Cheung, J.; Rudolph, M. J.; Burshteyn, F.; Cassidy, M. S.; Gary, E. N.; Love, J.; Franklin, M. C.; Height, J. J. Structures of human acetylcholinesterase in complex with pharmacologically important ligands. *J. Med. Chem.* **2012**, *55*, 10282−10286.
(37) Di, L.; Kerns, E. H.; Fan, K.; McConnell, O. J.; Carter, G. T. High throughput artificial membrane permeability assay for blood_/ brain barrier. *Eur. J. Med. Chem.* **2003**, *38*, 223−232.
(38) Hughes, J. D.; Blagg, J.; Price, D. A.; Bailey, S.; DeCrescenzo, G. A.; Devraj, R. V.; Ellsworth, E.; Fobian, Y. M.; Gibbs, M. E.; Gilles, R. W.; Greene, N.; Huang, E.; Krieger-Burke, T.; Loesel, J.; Wager, T.; Whiteley, L.; Zhang, Y. Physiochemical drug properties associated with in vivo toxicological outcomes. *Bioorg. Med. Chem. Lett.* **2008**, *18*, 4872−4875.
(39) Di, L.; Kerns, E. H.; Hong, Y.; Chen, H. Development and application of high throughput plasma stability assay for drug discovery. *Int. J. Pharm.* **2005**, *297*, 110−119.
(40) Pauli, G. F.; Chen, S.-N.; Simmler, C.; Lankin, D. C.; Godecke, T.; Jaki, B. U.; Friesen, J. B.; McAlpine, J. B.; Napolitano, J. G. Importance of purity evaluation and the potential of quantitative ^{1}H NMR as a purity assay. *J. Med. Chem.* **2014**, *57*, 9220−9231.
(41) Hebda, M.; Bajda, M.; Wieckowska, A.; Szałłaj, N.; Pasieka, A.; Panek, D.; Godyń, J.; Wichur, T.; Knez, D.; Gobec, S.; Malawska, B. Synthesis, molecular modelling and biological evaluation of novel heterodimeric, multiple ligands targeting cholinesterases and amyloid beta. *Molecules* **2016**, *21*, 410.
(42) Karthivashan, G.; Park, S. Y.; Kweon, M. H.; Kim, J.; Haque, M. E.; Cho, D. Y.; Kim, I. S.; Cho, E. A.; Ganesan, P.; Choi, D. K. Ameliorative potential of desalted *Salicornia europaea* L. extract in multifaceted Alzheimer's-like scopolamine-induced amnesic mice model. *Sci. Rep.* **2018**, *8*, No. 7174.
(43) Morris, R. G. Spatial localization does not depend on the presence of local cues. *Learn. Motivation* **1981**, *12*, 239−260.
(44) Kaur, S.; Kaur, A.; Singh, G.; Bhatti, R. *Mercurius solubilis* attenuates scopolamine-induced memory deficits and enhances the motor coordination in mice. *Int. J. Neurosci.* **2018**, *128*, 219−230.
(45) Molinspiration Calculation of Molecular Propertiers. https://www.molinspiration.com/ (accessed March 20, 2022).
(46) *PreADMET Program*; Bioinformatics and Molecular Design Research Centre: Seoul, South Korea, 2004 http://preadmet.bmdrc.org.

https://doi.org/10.1021/acsomega.3c09069
ACS Omega 2024, 9, 12896−12913